

Regulation of prefrontal excitatory neurotransmission by dopamine in the nucleus accumbens core

Wengang Wang¹, Dennis Dever¹, Janet Lowe¹, Granville P. Storey¹, Anita Bhansali¹, Emily K. Eck¹, Ioana Nitulescu¹, Jessica Weimer¹ and Nigel S. Bamford^{1,2}

¹Department of Neurology, University of Washington, Seattle, WA 98195, USA

²Departments of Pediatrics and Psychology, the Graduate Program in Neurobiology and Behavior, and Center on Human Development and Disability, University of Washington and Seattle Children's Hospital, Seattle, WA 98105, USA

Key points

- Dopamine's control over excitatory signals from the cortex to the nucleus accumbens is thought to underlie motor learning, behavioural reinforcement and drug dependence.
- In this study, we combined optical recordings of presynaptic release with whole-cell electrophysiology in CB₁ receptor-null mice and bacterial artificial chromosome (BAC) transgenic mice with fluorescently labelled D1 and D2 receptor-expressing neurons to identify the specific interactions between dopamine and glutamate signalling at individual cortical terminals within the nucleus accumbens core.
- Experiments showed that dopamine produces frequency-dependent filtering of low-probability release synapses. At low frequencies, D1 receptors excited striatal output neurons of the striatonigral and striatopallidal pathways, while D2 receptors specifically inhibited neurons of the striatopallidal pathway. At higher frequencies, the dopamine-dependent release of adenosine and endocannabinoids promoted further temporal filtering of cortical signals entering both output pathways.
- These results help us understand how dopamine provides frequency and temporal filtering of cortical information by promoting activity through the striatonigral pathway, while inhibiting weak signals.

Abstract Interactions between dopamine and glutamate signalling within the nucleus accumbens core are required for behavioural reinforcement and habit formation. Dopamine modulates excitatory glutamatergic signals from the prefrontal cortex, but the precise mechanism has not been identified. We combined optical and electrophysiology recordings in murine slice preparations from CB₁ receptor-null mice and green fluorescent protein hemizygotic bacterial artificial chromosome transgenic mice to show how dopamine regulates glutamatergic synapses specific to the striatonigral and striatopallidal basal ganglia pathways. At low cortical frequencies, dopamine D1 receptors promote glutamate release to both D1 and D2 receptor-expressing medium spiny neurons while D2 receptors specifically inhibit excitatory inputs to D2 receptor-expressing cells by decreasing exocytosis from cortical terminals with a low probability of release. At higher cortical stimulation frequencies, this dopaminergic modulation of presynaptic activity is occluded by adenosine and endocannabinoids. Glutamatergic inputs to both D1 and D2 receptor-bearing medium spiny neurons are inhibited by adenosine, released upon activation of NMDA and AMPA receptors and adenylyl cyclase in D1 receptor-expressing cells. Excitatory inputs to D2 receptor-expressing cells are specifically inhibited by endocannabinoids, whose release is dependent on D2 and group 1 metabotropic glutamate receptors. The convergence of excitatory and inhibitory modulation of corticoaccumbal activity by dopamine, adenosine

and endocannabinoids creates subsets of corticoaccumbal inputs, selectively and temporally reinforces strong cortical signals through the striatonigral pathway while inhibiting the weak, and may provide a mechanism whereby continued attention might be focused on behaviourally salient information.

(Resubmitted 24 April 2012; accepted 14 May 2012; first published online 21 May 2012)

Corresponding author N. S. Bamford: University of Washington, Department of Neurology, Box 356465, RR650, 1955 NE Pacific Street, Seattle, WA 98195, USA. Email: bamford@u.washington.edu

Abbreviations AMPAR, AMPA receptor; AMPH, amphetamine; BAC, bacterial artificial chromosome; D1R+, D1 receptor-expressing MSN; D2R+, D2 receptor-expressing MSN; eEPSC, evoked EPSC; EGFP, enhanced green fluorescent protein; LTD, long-term depression; mEPSC, miniature EPSC; mGluR, metabotropic glutamate receptor; MSN, medium spiny neuron; NAc, nucleus accumbens core; NMDAR, NMDA receptor; PFC, prefrontal cortex; PKA, protein kinase A; PPR, paired-pulse ratio; R, receptor; sEPSC, spontaneous EPSC; Veh, vehicle; VTA, ventral tegmentum.

Introduction

The neocortex refines movements and goal-directed behaviours through basal ganglia circuits that contribute feedback and feed-forward integrative signalling (Albin *et al.* 1989). Excitatory glutamatergic signals from neurons in the prefrontal cortex (PFC) and dopaminergic projections from neurons in the ventral tegmentum (VTA) enter the nucleus accumbens core (NAc) to form synapses on medium spiny neurons (MSNs). Dopamine released by salient behavioural stimuli or amphetamine (Pennartz *et al.* 1994; Sulzer, 2011) diffuses into the synaptic cleft where it differentially regulates the excitability of D1-class dopamine receptor (D1R)-expressing MSNs, which constitute the 'direct' striatonigral pathway that initiates movements and behaviours, and D2-class dopamine receptor (D2R)-expressing MSNs, which form the 'indirect' striatopallidal pathway that suppresses competing actions (Pennartz *et al.* 1994; Nicola *et al.* 2000).

Regulation of excitatory signals by dopamine and other neuromodulators, including adenosine and endocannabinoids, is considered necessary for the establishment of reward and attention (Harvey & Lacey, 1996; Kalivas & Volkow, 2005; Bamford *et al.* 2008; Pan *et al.* 2008) and alterations in their availability are thought to underlie numerous neuropsychological disorders including Parkinsonism (Bamford & Cepeda, 2009; Cepeda *et al.* 2010), schizophrenia (Goto & Grace, 2007), and drug dependence (Kalivas & Volkow, 2005). However, the mechanism by which this modulation develops in the NAc remains unclear. Electrophysiological recordings have shown that dopamine can impede corticoaccumbal activity through presynaptic D1 (Harvey & Lacey, 1996; Nicola *et al.* 1996; Nicola & Malenka, 1997) and D2 receptors (O'Donnell & Grace, 1994; Brady & O'Donnell, 2004), or through adenosine (Harvey & Lacey, 1997; Dunwiddie & Masino, 2001) and endocannabinoids (Grueter *et al.* 2010). Thus, how dopamine modulates corticoaccumbal neurotransmission

remains unsettled, although this issue is paramount to understanding striatal function.

To gain an understanding of how dopamine controls cortical information entering the striatonigral and striatopallidal pathways within the NAc, we combined presynaptic optical approaches with postsynaptic electrophysiology in CB₁ receptor (CB₁R)-null mice (CB₁^{-/-}) and in hemizygotic bacterial artificial chromosome (BAC) transgenic mice expressing the reporter enhanced green fluorescent protein (EGFP) under the control of the D1 and D2 dopamine receptor promoters (Drd1-EGFP and Drd2-EGFP). The goals of this study were first to identify frequency- and stimulation-dependent interactions between dopamine and glutamate signalling at individual cortical terminals within the NAc and second to determine how adenosine and endocannabinoids channel information through striatonigral and striatopallidal pathways.

Methods

Ethical approval

All experimental procedures were approved by the Institutional Animal Care and Use Committee at the University of Washington. Male mice aged 4–9 weeks were housed with a 12 h light–dark cycle with *ad libitum* access to food and water and were anaesthetized with Nembutal (120 mg kg⁻¹ i.p.) or ketamine (650 mg kg⁻¹ i.p.) with xylazine (44 mg kg⁻¹ i.p.) prior to killing. C57BL/6 mice ($n = 202$) were obtained from The Jackson Laboratory (Bar Harbor, ME, USA). CB₁^{-/-} ($n = 12$) and wild-type (WT) littermates (CB₁^{+/+}; $n = 10$), generated as described on a C57BL/6 background (Marsicano *et al.* 2003), were a kind gift from Dr Nephi Stella, University of Washington, Seattle. Hemizygous Drd1 ($n = 54$) and Drd2 ($n = 40$) EGFP BAC transgenic mice were generated as described on a C57BL/6 background (Cepeda *et al.* 2008) and mice used for breeding were a kind gift from Dr Michael Levine, University of California, Los Angeles, CA, USA.

Optical imaging with FM1-43

Optical recordings of cortical afferents in the motor striatum were performed as described (Bamford *et al.* 2004a). Sagittal sections 250 μm thick containing the PFC and NAcore were cut using a vibrating blade microtome and recovered for 1 h in carbogenated (95% O_2 , 5% CO_2) ACSF containing (in mM): NaCl 109, KCl 5, NaHCO_3 35, NaH_2PO_4 1.25, Hepes 20, MgCl_2 1.2, CaCl_2 2, glucose 10 (pH 7.3–7.4, 295–305 mosmol l^{-1}) at room temperature. Experiments were performed on slices obtained at an interaural distance range of 0.72 mm to 1.44 mm from midline. During the experiment, slices were held in a RC-27L incubation chamber (56 $\mu\text{l mm}^{-1}$; Warner Instruments, Hamden, CT, USA) and were perfused with ACSF at 2–3 ml min^{-1} . To ensure equilibrium, sections were exposed to pharmacological agents for 10 min before unloading. Drugs were obtained from Sigma-Aldrich (St Louis, MO, USA) or Tocris Bioscience (Bristol, UK).

The endocytic tracer FM1-43 (*N*-[3-(triethylammonio)propyl]-4-(4-dibutylaminostyryl)pyridinium dibromide; Molecular Probes; 8 μM) was loaded into corticoaccumbal terminals by stimulating the PFC at 10 Hz for 10 min with 400 μA , 200 μs pulses via a twisted tungsten bipolar electrode. The electrode was placed over the dorsal PFC that preferentially projects to the NAcore (Gorelova & Yang, 1997). This loading method ensures that changes in release of FM1-43 are not due to inadequate FM1-43 loading of the recycling synaptic vesicle pool (Bamford *et al.* 2004b; Joshi *et al.* 2009). As FM1-43 destaining generally followed first-order kinetics (Joshi *et al.* 2009), corticoaccumbal release was characterized by the half-time of destaining ($t_{1/2}$), defined as the time required for terminal fluorescence to decay to half of its initial value.

Following terminal loading, slices were superfused in ADVASEP-7 (1 mM; CyDex, Overland Park, KS, USA) for 2 min to remove adventitious staining. For stimulation-dependent destaining, pulse trains were again delivered to the dorsal PFC. ADVASEP-7 (100 μM) was used during unloading to prevent recurrent endocytosis of dye into synaptic terminals. Few puncta were labelled in the absence of stimulation (Joshi *et al.* 2009) or following a cut between the cortex and striatum and no destaining occurred upon restimulation. Electrical stimulation was provided by a Grass Stimulator (West Warwick, RI, USA) through a stimulation isolator (AMPI, Jerusalem, Israel) and monitored by a Tektronix TDS 3014B digital oscilloscope (Beaverton, OR, USA).

Image acquisition and analysis

Fluorescent corticoaccumbal terminals in the NAcore were visualized using an LSM 510 NLO multiphoton laser-scanning microscope equipped with a titanium-sapphire laser (excitation 810 nm/emission

625 nm) and a 40 \times inverted oil objective (Zeiss). Images were captured in 8-bit, 123 $\mu\text{m} \times 123 \mu\text{m}$ regions of interest (ROI) at 512 pixel \times 512 pixel resolution and acquired at 22.5 s intervals using Zeiss LSM 510 software. To compensate for *z*-axis shift, a *z*-series of five images, separated by 1 μm in the *z*-axis, was obtained for each imaging period. The time series of images was analysed for changes in presynaptic terminal fluorescence using ImageJ (Wayne Rosband, National Institutes of Health, Rockville, MD, USA) and custom software written in Interactive Data Language (IDL; Research Systems, Boulder, CO, USA) (Bamford *et al.* 2004b). Fluorescent puncta, 0.5–1.5 μm in diameter, were identified in the NAcore. The criteria for punctum inclusion were (1) spherical shape, (2) fluorescence 2 standard deviations above the background, and (3) stimulation-dependent destaining. The IDL software aligned and combined the five image *z*-series for each time interval and the overall intensity of the FM1-43 fluorescence was measured over the course of the time series. ImageJ was used to subtract background fluorescence of the tissue from the fluorescence intensity of each individual punctum. The results were then normalized by the maximal puncta fluorescence just prior to application of destaining stimulation. The half-time of fluorescence intensity decay during destaining ($t_{1/2}$) was determined using a software algorithm written on SigmaPlot software (Systat Software Inc., San Jose, CA, USA). Nearness of fit to first-order kinetics was determined using $A = 100 \times \exp(\ln(0.5) \times t/t_{1/2})$, an integrated form of the first-order kinetics equation: $-dA/dt = kA$.

Electrophysiology

Electrophysiological recordings in MSNs from mice were performed, as described (Bamford *et al.* 2008), and standard techniques were used to prepare slices for electrophysiology (Bamford *et al.* 2004b). Brains were dissected and placed in ice-cold, carbogenated low Ca^{2+} ACSF containing (in mM): NaCl 130, KCl 3, NaHCO_3 26, NaH_2PO_4 1.25, MgCl_2 5, CaCl_2 1 and glucose 10. Sagittal slices (300 μm) were prepared on a vibrating blade microtome then transferred to an incubating chamber containing carbogenated background ACSF containing (in mM): NaCl 124, KCl 5, NaHCO_3 26, NaH_2PO_4 1.25, MgCl_2 2, CaCl_2 2 and glucose 10 (pH 7.2–7.4, 290–310 mosmol l^{-1}) at room temperature. After 1 h, slices were placed on the stage of a Zeiss Axioskop FS microscope and submerged in continuously flowing carbogenated background ACSF (3 ml min^{-1}) at room temperature.

Whole-cell patch clamp recordings in voltage clamp mode were obtained from MSNs ($n = 395$) visualized in slices with the aid of infrared videomicroscopy coupled with differential interference contrast optics and

fluorescent filters optimized to detect EGFP fluorescence and infrared light. MSNs were identified by somatic size ($\sim 8\text{--}12\ \mu\text{m}$) and typical passive basic membrane properties (membrane resistance $212 \pm 9\ \text{M}\Omega$, membrane capacitance $100 \pm 2\ \text{pF}$ and time constant $1.6 \pm 0.03\ \text{ms}$) (Joshi *et al.* 2009). Cell identification was confirmed by labelling with 1% biocytin, according to published protocols (Cepeda *et al.* 2001). The series resistance of each cell was $<20\ \text{M}\Omega$ ($15.4 \pm 0.3\ \text{M}\Omega$). Electrophysiological properties were monitored throughout the recording and cells were removed from the analysis if the series resistance changed by $>20\%$. For voltage clamp recordings, the patch pipette ($4\text{--}6\ \text{M}\Omega$) contained the following internal solution (in mM): caesium methanesulfonate 125, KCl 3, NaCl 4, MgCl_2 1, MgATP 5, EGTA 5, Hepes 8, Tris-GTP 1, di-sodium phosphocreatine 10, leupeptin 0.1 and *N*-(2,6-dimethylphenylcarbamoylmethyl) triethylammonium bromide 4 (QX-314; pH 7.2–7.3, $270\text{--}280\ \text{mosmol l}^{-1}$). In some experiments, the cAMP inhibitor Rp-cAMPS ($400\ \mu\text{M}$) was added to the internal solution. For current-clamp recordings, the patch pipette ($4\text{--}6\ \text{M}\Omega$) contained the following internal solution (in mM): potassium gluconate 112.5, KCl 17.5, NaCl 4, MgCl_2 1, CaCl_2 0.5, EGTA 5, Hepes 10, NaGTP 1, K_2ATP 5 (pH 7.2–7.3, $270\text{--}280\ \text{mosmol l}^{-1}$). EPSCs were isolated by blocking GABA-A receptors with picrotoxin ($50\ \mu\text{M}$) or with bicuculline ($10\ \mu\text{M}$). In addition, cells were held at $-70\ \text{mV}$ to further minimize the contribution of GABA-A mediated events and that of voltage-gated conductances.

Excitatory postsynaptic currents (EPSCs) were evoked by electrical stimulation of the deep cortical layers of the dorsal PFC at stimulation strengths adjusted to $1.5\times$ threshold ($1.5 \pm 0.1\ \text{mA}$). The stimulating electrodes were of the same type of bipolar tungsten electrode used in the optical studies and both stimulating and recording electrodes were placed in the same locations described in the imaging experiments. Paired current pulses ($200\ \mu\text{s}$ duration) delivered at 20 Hz were presented every 30 s. Evoked (e) EPSC amplitudes were averaged and compared before and during bath application of the receptor ligand. Paired-pulse ratios were determined by dividing the amplitude of the second pulse by that of the first pulse and then multiplying by 100. Cells demonstrating eEPSCs with variable latencies or prolonged durations, suggesting polysynaptic responses, were rejected from analysis.

Miniature (m) EPSCs were recorded in gap free mode with the Na^+ channel blocker TTX ($1\ \mu\text{M}$) for 90 s before and during bath-application of a receptor ligand. Spontaneous (s) EPSCs were recorded without TTX. For some experiments, sEPSCs were recorded following conditioning stimuli. In these cells, the stimulus current threshold required to evoke an EPSC was determined using six single cortical pulses applied every 30 s. Conditioning stimuli, consisting of two paired-pulses at 20 Hz, were then presented three

times with a 30 s interval between stimulation trains. The brain slices were then exposed to the receptor ligand and sEPSCs were again observed for 90 s. The membrane current was filtered at 1 kHz and digitized at $100\ \mu\text{s}$ using Clampfit 10.1 (Molecular Devices, Inc., Sunnyvale, CA, USA). Spontaneous synaptic events were analysed off-line using the Mini Analysis Program (Synaptosoft, Leonia, NJ, USA). The threshold amplitude for the detection of an event was adjusted to at least 2 times above root mean square noise level ($\sim 2\text{--}3\ \text{pA}$ at $-70\ \text{mV}$). Synaptic events could be prevented by adding the AMPA receptor (AMPA) antagonist 2,3-dihydroxy-6-nitro-7-sulfamoyl-benzo[f]quinoxaline-2,3-dione (NBQX; $10\ \mu\text{M}$) to the bath solution, indicating that they arose from activation of glutamatergic receptors.

Data analysis

Values given in the text and in the figures are means \pm SEM. Differences in mean values, derived from 3–14 slices from 3–9 mice, were assessed with the non-parametric Mann–Whitney *U* test, Student's paired *t* test (two groups) or appropriate ANOVAs (multiple groups) followed by multiple comparisons using a Bonferroni adjustment. For optical studies, destaining was compared using the *F* test, population distributions were compared using the Kolmogorov–Smirnov test and changes in terminal subpopulations were also determined graphically using normal probability plots by comparing release half-times of individual terminals. For electrophysiological experiments, data was compared using a Student's paired *t* test before and 5 to 7.5 min after ligand perfusion. Differences analysed by Statistica (StatSoft, Tulsa, OK, USA) were considered significant if $P < 0.05$.

Online Supplemental Material

Supplementary methods, figures and references are provided. Supplementary Methods and Fig. S1 illustrate the fractional destaining of FM1-43 at 1 Hz through 20 Hz with and without the dopamine releaser amphetamine. Supplementary Figs S2–S7 show how amphetamine, dopamine, endocannabinoid and glutamate receptors modify subpopulations of corticoaccumbal terminals.

Results

Dopamine and endocannabinoids promote frequency-dependent filtering at presynaptic corticoaccumbal terminals

Exocytosis from PFC terminals within the NAc core was directly measured using the endocytic tracer FM1-43 combined with multiphoton confocal microscopy

in murine sagittal slices (Fig. 1A and B). Bipolar stimulation of layers V–VI of the dorsal PFC produced endocytosis of FM1-43 dye into recycling synaptic vesicles (Fig. 1B–D). Multiphoton optical recordings in the NAcore revealed fluorescent puncta (diameter = $1.1 \pm 0.1 \mu\text{m}$; mean \pm SEM; $n = 11$ puncta) distinctive of corticostriatal afferents that, upon re-stimulation, decreased in a manner approximating first-order kinetics ($r^2 > 0.973$; $P < 0.001$, F test), characteristic of regulated synaptic vesicle fusion (Bamford *et al.* 2004b) (Fig. 1D–F). Corticoaccumbal release was characterized by the half-time of destaining ($t_{1/2}$), defined as the time required for terminal fluorescence to decay to half of its initial value.

Stimulation of the PFC in slices from WT mice at frequencies of 1 Hz ($n = 104$ puncta), 10 Hz ($n = 136$), and 20 Hz ($n = 330$) produced a corresponding increase in terminal release reflected by a decrease in the half-time of FM1-43 destaining ($t_{1/2} = 305$ s at 1 Hz, $t_{1/2} = 245$ s at 10 Hz, and $t_{1/2} = 207$ s at 20 Hz; $F_{(2,567)} = 28$, $P < 0.001$, ANOVA) (Fig. 1G and I). Little FM1-43 destaining occurred in the absence of cortical stimulation ($n = 80$) and destaining was calcium dependent, as bath application of the calcium channel blocker cadmium ($200 \mu\text{M}$; $n = 99$) prevented release of the dye (Fig. 1G), consistent with vesicular exocytosis.

To determine if dopamine might alter corticoaccumbal exocytosis, we recorded FM1-43 destaining in the presence of amphetamine ($10 \mu\text{M}$), which raises striatal dopamine concentrations to $\sim 6 \mu\text{M}$ (Bamford *et al.* 2004b). Compared to vehicle, amphetamine had little effect on FM1-43 release in slices from WT mice at stimulation frequencies of 1 Hz ($t_{1/2} = 308$ s; $n = 103$) and 10 Hz ($t_{1/2} = 268$ s; $n = 97$), but decreased the half-time of FM1-43 release at 20 Hz stimulation ($t_{1/2} = 264$ s; $n = 193$; $F_{(4,1442)} = 2.3$, $P = 0.05$, 2-way ANOVA for interaction between frequency and amphetamine) by diminishing the fractional destaining of FM1-43 by 42% (Fig. 1I and Fig. S1).

One advantage of these optical recordings is that the kinetics of individual presynaptic terminals can be observed. When individual terminal half-times are presented in a normal probability plot, where the x -axis indicates the standard deviation from the median value, a straight line indicates a normally distributed population (Bamford *et al.* 2004b). At 20 Hz stimulation frequency, amphetamine specifically depressed release from a subset of terminals with a low probability of release (Fig. 1J and Supplementary Fig. S2).

We determined if the apparent lack of response to amphetamine at lower stimulation frequencies might be attributed to the differential effects of amphetamine acting through D1 and D2 dopamine receptors. With bath application of the D1R agonist SKF38393 ($10 \mu\text{M}$), the half-time of dye release remained constant with an increase

in stimulation frequency ($t_{1/2} = 251$ s at 1 Hz, $n = 97$; $t_{1/2} = 262$ s at 10 Hz, $n = 122$, and $t_{1/2} = 270$ s at 20 Hz, $n = 266$) so that compared to vehicle, the D1R agonist was excitatory at 1 Hz ($P < 0.001$, Mann–Whitney U test) but inhibitory at 20 Hz ($P < 0.001$, Mann–Whitney U test) (Fig. 1K). Conversely, the D2R agonist quinpirole ($0.5 \mu\text{M}$) had little effect at 1 Hz ($t_{1/2} = 306$ s, $n = 96$) but progressively depressed release at higher frequencies of 10 Hz ($t_{1/2} = 302$ s; $P < 0.001$, $n = 86$, Mann–Whitney U test) and 20 Hz ($t_{1/2} = 248$ s; $P < 0.001$, compared to vehicle, $n = 80$, Mann–Whitney U test) (Fig. 1L). Similar to amphetamine, both SKF38393 and quinpirole modulated terminals with a low probability of release (Supplementary Fig. S3) and the combined responses from SKF38393 and quinpirole at stimulation frequencies of 1 Hz to 20 Hz ($t_{1/2} = 291$ s at 1 Hz, $n = 193$; $t_{1/2} = 283$ s at 10 Hz, $n = 208$ and $t_{1/2} = 280$ s at 20 Hz, $n = 186$) were similar to those following amphetamine (Fig. 1M).

Stimulation frequencies in excess of 20 Hz caused a progressive reduction in corticoaccumbal exocytosis in the absence of amphetamine ($t_{1/2} = 207$ s at 20 Hz; $t_{1/2} = 236$ s at 30 Hz, $n = 105$, and $t_{1/2} = 252$ s at 40 Hz, $n = 88$; $F_{(2,520)} = 17$, $P < 0.001$, ANOVA), such that amphetamine had no effect on presynaptic release at stimulation frequencies of 30 Hz ($t_{1/2} = 259$ s; $n = 147$) and 40 Hz ($t_{1/2} = 265$ s; $n = 148$) (Fig. 1H–I and Supplementary Fig. S2). Consistent with prior reports (Yin & Lovinger, 2006), presynaptic inhibition by amphetamine at stimulation frequencies above 10 Hz was dependent on endocannabinoids, since amphetamine had no effect on release in slices from $\text{CB}_1^{-/-}$ mice ($t_{1/2} = 305$ s at 1 Hz, $n = 78$; 239 s at 10 Hz, $n = 91$; 208 s at 20 Hz, $n = 102$; 189 s at 30 Hz, $n = 71$; 177 s at 40 Hz, $n = 77$) (Fig. 1I). Furthermore, while FM1-43 release in slices from $\text{CB}_1^{-/-}$ mice increased with stimulation frequencies of 1 Hz to 20 Hz ($t_{1/2} = 285$ s at 1 Hz, $n = 76$; $t_{1/2} = 236$ s at 10 Hz, $n = 162$; $t_{1/2} = 201$ s at 20 Hz; $n = 114$; $F_{(2,294)} = 9$, $P < 0.001$, compared with vehicle in WT mice, ANOVA) (Fig. 1I), higher stimulation frequencies of 30 Hz and 40 Hz reduced exocytosis from most terminals in slices from WT mice but not in slices from $\text{CB}_1^{-/-}$ mice ($t_{1/2} = 200$ s at 30 Hz, $n = 81$ and $t_{1/2} = 206$ s at 40 Hz, $n = 72$, $P < 0.001$, Mann–Whitney U test) (Fig. 1I and Supplementary Fig. S4), suggesting that very high stimulation frequencies can release endocannabinoids in the absence of dopamine.

Presynaptic inhibition through adenosine is dependent on D1, NMDA and AMPA receptors

Since presynaptic filtering by amphetamine was generated at 20 Hz, we used this stimulation frequency to determine how corticoaccumbal inhibition was produced through D1Rs. Similar to amphetamine, the D1R agonist SKF38393

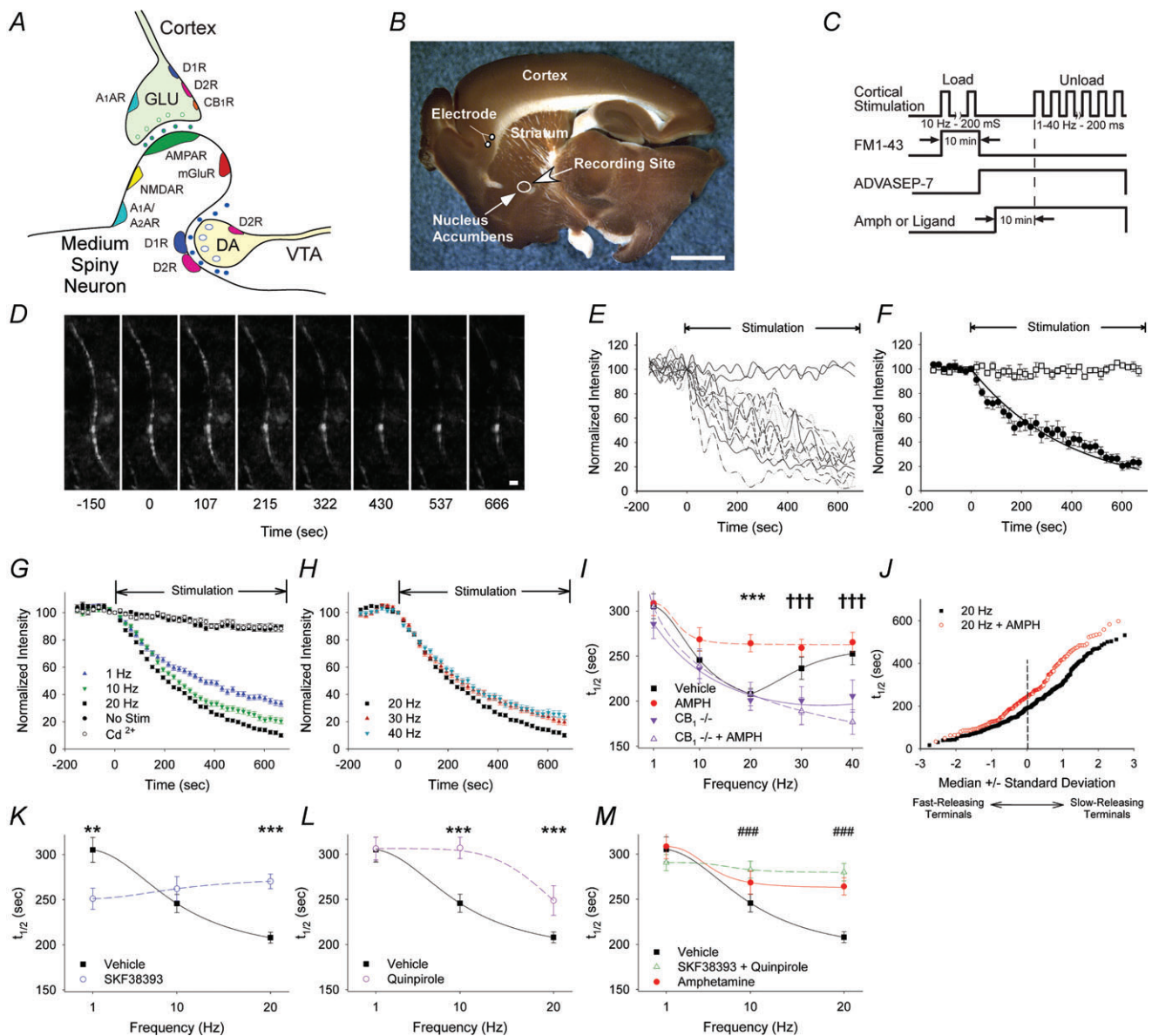


Figure 1. Amphetamine and endocannabinoids produce frequency-dependent filtering at cortico-accumbal terminals

A, cartoon of the basic 'striatal microcircuit'. GLU, glutamatergic afferent; VTA, ventral tegmental area; DA, dopamine afferent; mGluR, metabotropic glutamate receptor; D, dopamine receptor; A₁R and A₂R, adenosine receptor; CB₁, cannabinoid receptor. B, a sagittal corticoaccumbal slice stained with FM1-43 and 3,3'-diaminobenzidine shows the stimulation and recording regions. Corticoaccumbal terminals from the PFC were stimulated with a bipolar electrode. Two-photon images of corticoaccumbal terminals and electrophysiological recordings in MSNs were obtained within the NAc core (circle within the striatum). Bar, 3 mm. C, protocol for loading and destaining corticoaccumbal terminals with FM1-43. D, stimulation of the PFC in the presence of FM1-43 created labelled puncta, sometimes seen in *en passant* arrays. Re-stimulation of the PFC at 20 Hz resulted in activity-dependent destaining of most puncta. Stimulation began at $t = 0$. Bar, 2 μm . E, time-intensity analysis of fluorescent puncta along the axon array, shown in panel D, during unloading demonstrates differential release kinetics. The plateau lines on the graph represent optical measurements from non-destaining fluorescent puncta. F, mean \pm SEM fluorescence intensity of destaining and non-destaining puncta shown in panel E. Curve demonstrates exponential fitting for first-order kinetics. G, stimulation of the PFC at 1 Hz, 10 Hz and 20 Hz produced a frequency-dependent increase in FM1-43 destaining reflected by a decrease in FM1-43 destaining. Little FM1-43 destaining occurred when no stimulation was applied or when cadmium (Cd^{2+}) was added to the bath. H, PFC stimulation frequencies of 30 Hz and 40 Hz progressively reduced exocytosis from corticoaccumbal terminals. I, mean destaining half-times ($t_{1/2}$) of FM1-43 release in slices from WT and CB₁^{-/-} mice perfused in vehicle or amphetamine (AMPH). * $P < 0.05$, ** $P < 0.01$, *** $P < 0.001$, amphetamine compared with vehicle

increased FM1-43 destaining ($t_{1/2} = 270$ s for a SKF38393, $n = 193$ puncta *vs.* $t_{1/2} = 207$ s for vehicle, $n = 330$; $P < 0.001$, Mann–Whitney *U* test) (Fig. 2A and B), by inhibiting terminals with the lowest probability of release (Supplementary Fig. S5). The D1R antagonist SCH23390 ($10 \mu\text{M}$) did not change exocytosis ($t_{1/2} = 183$ s, $n = 163$; $P = 0.1$, compared to vehicle, Mann–Whitney *U* test) (Fig. 2A and B) and as expected, blocked inhibition by the D1R agonist SKF38393 ($t_{1/2} = 213$ s, $n = 90$; $P = 0.1$, compared to vehicle, Mann–Whitney *U* test) (not shown). While the addition of SCH23390 to amphetamine accelerated FM1-43 destaining ($t_{1/2} = 237$ for amphetamine with SCH23390, $n = 163$; $P = 0.02$, compared to amphetamine alone, Mann–Whitney *U* test), it only partially blocked inhibition by amphetamine ($P = 0.03$, compared to vehicle, Mann–Whitney *U* test) (Fig. 2A and B), confirming that dopamine-mediated inhibition of corticoaccumbal activity occurred in part, but not entirely through D1Rs.

D1Rs have been shown to promote adenosine efflux and produce inhibition of glutamate release via A_1 adenosine receptors (A_1 Rs) (Harvey & Lacey, 1997) that are located on presynaptic corticoaccumbal terminals (Ciruela *et al.* 2006). Consistent with these reports, the receptor agonist adenosine ($60 \mu\text{M}$) inhibited corticoaccumbal release ($t_{1/2} = 251$ s for adenosine, $n = 112$; $P = 0.002$, compared to vehicle, Mann–Whitney *U* test) (Fig. 2C and D) and similar to the D1R agonist, reduced exocytosis from terminals with a low probability of release (Supplementary Fig. S5). The selective A_1 R antagonist 8-cyclopentyl-1,3-dipropylxanthine (DPCPX; 500 nM) alone did not alter FM1-43 destaining ($t_{1/2} = 212$, $n = 104$; $P = 0.1$, compared to vehicle, Mann–Whitney *U* test), but it prevented presynaptic depression caused by the D1R agonist SKF38393 ($t_{1/2} = 218$ s for SKF38393 with DPCPX, $n = 154$; $P = 0.5$, compared to vehicle, Mann–Whitney *U* test) (Fig. 2C and D), suggesting that D1R activation is required for any substantial adenosine production that would modify FM1-43 destaining.

We determined if presynaptic inhibition by D1Rs was dependent on NMDA receptor (NMDAR) activation. Bath application of the NMDAR antagonist 2-amino-5-phosphonopentanoic acid (APV; $50 \mu\text{M}$) prevented inhibition caused by SKF38393 ($t_{1/2} = 214$ s

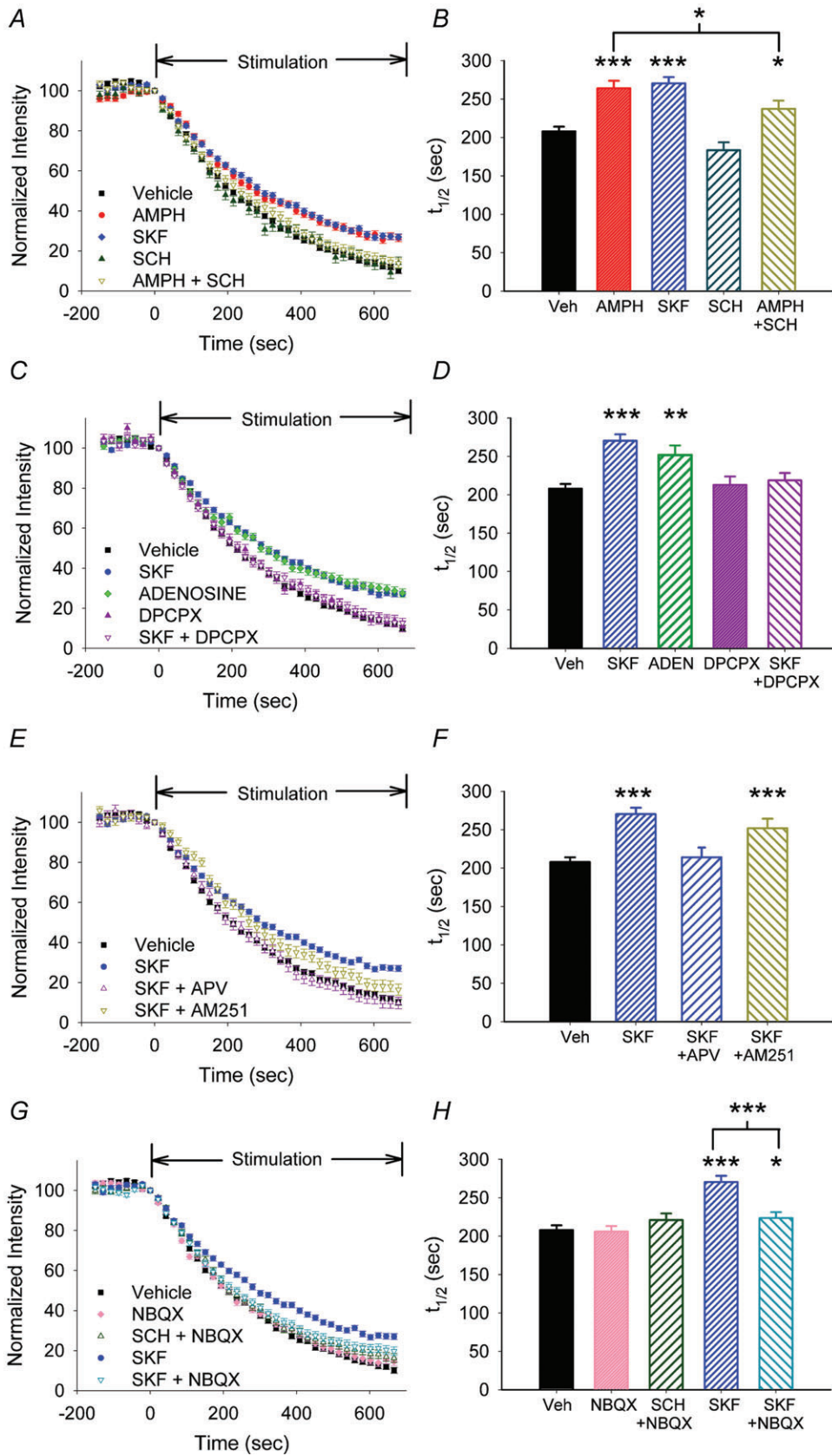
for SKF38393 with APV, $n = 266$; $P = 0.5$, compared with vehicle, Mann–Whitney *U* test) (Fig. 2E and F and Supplementary Fig. S5), suggesting that D1Rs can augment NMDAR-dependent signalling (Levine *et al.* 1996) and release adenosine (Manzoni *et al.* 1994; Harvey & Lacey, 1997). We suspected that AMPARs might also facilitate presynaptic inhibition by D1Rs, as they can enable NMDAR activation by elevating cellular resting membrane potentials (Cherubini *et al.* 1988). Corticoaccumbal destaining half-times remained unchanged in the presence of the AMPAR antagonist NBQX ($10 \mu\text{M}$; $t_{1/2} = 206$ s for NBQX; $n = 205$; $P = 0.5$, compared to vehicle, Mann–Whitney *U* test) and NBQX had no effect on release when combined with the D1R antagonist SCH23390 ($t_{1/2} = 220$ s for NBQX with SCH23390; $n = 122$; $P = 0.1$, compared with NBQX alone, Mann–Whitney *U* test) (Fig. 2G and H and Supplementary Fig. S5). However, NBQX diminished ($t_{1/2} = 224$ s for SKF38393 with NBQX; $n = 159$; $P < 0.001$, compared to SKF38393, Mann–Whitney *U* test), but did not completely prevent, inhibition caused by SKF38393 ($P = 0.02$, compared to vehicle, Mann–Whitney *U* test) (Fig. 2G and H). Thus, co-activation of D1, NMDA and AMPA receptors increased adenosine receptor activity to reduce destaining kinetics.

Endocannabinoids can also regulate presynaptic activity (Yin & Lovinger, 2006). However, presynaptic inhibition by D1Rs was independent of endocannabinoid signalling, as the CB_1 R antagonist AM251 ($1 \mu\text{M}$) with SKF38393 did not change FM1-43 release ($t_{1/2} = 251$ s for SKF38393 with AM251, $n = 72$ *vs.* 270 s for SKF38393 alone; $P = 0.1$, Mann–Whitney *U* test) (Fig. 2E and F and Supplementary Fig. S5).

Presynaptic inhibition through endocannabinoids is dependent on D2 and group 1 metabotropic glutamate receptors (mGluRs)

Next, we examined how D2Rs modulate excitatory inputs to the NAc core. The D2R agonist quinpirole decreased FM1-43 destaining ($t_{1/2} = 249$ s for quinpirole; $n = 80$ puncta; $P = 0.01$, compared to vehicle, Mann–Whitney *U* test) (Fig. 3A and B), primarily by inhibiting

and $\dagger\dagger\dagger P < 0.001$ for vehicle or amphetamine, compared with data obtained from $CB_1^{-/-}$ mice, Mann–Whitney *U* test. *J*, normal probability plot comparison of individual half-times of release in slices from WT mice shows that amphetamine reduces FM1-43 release from terminals with lowest probability of release (e.g. those with the highest $t_{1/2}$). *K*, distribution of mean $t_{1/2}$ of release for slices from WT mice exposed to vehicle or the D1R agonist SKF38393 (SKF) at 1, 10 and 20 Hz. For panels *K* and *L*, $**P < 0.01$, $***P < 0.001$, Mann–Whitney *U* test. *L*, distribution of mean $t_{1/2}$ of release for slices from WT mice exposed to vehicle or the D2R agonist quinpirole (QUIN) at 1, 10 and 20 Hz. *M*, distribution of mean $t_{1/2}$ of release in slices from WT mice exposed to vehicle, amphetamine or to the combination of SKF38393 and quinpirole at 1, 10 and 20 Hz. $####P < 0.001$ for SKF38393 with quinpirole, compared with vehicle, Mann–Whitney *U* test.



cortical terminals with the lowest probability of release (Supplementary Fig. S6). The D2R antagonist sulpiride (10 μM) alone had no effect on release ($t_{1/2} = 211$ s; $n = 60$; $P = 0.5$, compared to vehicle, Mann–Whitney U test) (Fig. 3A and B) and as expected, blocked inhibition by quinpirole ($t_{1/2} = 213$ s for quinpirole with sulpiride; $n = 45$; $P = 0.5$, compared to vehicle, Mann–Whitney U test) (not shown). However, sulpiride only partially prevented corticoaccumbal inhibition by amphetamine ($t_{1/2} = 220$ s for amphetamine with sulpiride; $n = 146$; $P = 0.03$, compared to vehicle, Mann–Whitney U test) (Fig. 3A and B). Inhibition by amphetamine required both D1 and D2 receptors since it was prevented only by both D1 and D2 receptor antagonists ($t_{1/2} = 201$ s for amphetamine in combination with SCH23390 and sulpiride; $n = 228$; $P = 0.5$, compared to vehicle, Mann–Whitney U test) (Fig. 3D). The actions of D1 and D2 receptors on corticoaccumbal activity were independent, with modulation by amphetamine representing a complementary balance between their individual responses (Fig. 1M).

We determined if inhibition by D2Rs might occur through cannabinoid receptors located on presynaptic glutamatergic terminals in the NAc core (Pickel *et al.* 2006). The CB₁R agonist WIN55-2,2 (2 μM) inhibited FM1-43 destaining ($t_{1/2} = 271$ s; $n = 81$; $P < 0.001$, compared to vehicle, Mann–Whitney U test) to a similar extent as the D2R agonist quinpirole ($t_{1/2} = 248$ s; $n = 80$; $P = 0.4$, compared to WIN55-2,2, Mann–Whitney U test) (Fig. 3E and F). The CB₁R antagonist AM251 prevented inhibition by quinpirole ($t_{1/2} = 184$ s for quinpirole with AM251; $n = 72$; $P = 0.2$, compared to vehicle, Mann–Whitney U test) and increased release from a broad population of terminals in otherwise untreated slices ($t_{1/2} = 173$ s for AM251; $n = 43$; $P = 0.002$, compared with vehicle, Mann–Whitney U test) (Fig. 3E and F and Supplementary Fig. S6), suggesting that MSN activation produces some tonic endocannabinoid efflux that is independent of D2R activation.

In the ventral (Grueter *et al.* 2010) and dorsal striatum (Yin & Lovinger, 2006) and in the VTA (Pan *et al.* 2008),

presynaptic inhibition through CB₁R is dependent on activation of group 1 mGluRs. Consistent with these reports, quinpirole's inhibition at presynaptic terminals was suppressed by the mGluR₁ antagonist 7-hydroxyiminocyclopropan[b]chromen-1 α -carboxylic acid ethyl ester (CPCCOEt; 40 μM ; $t_{1/2} = 211$ s for quinpirole with CPCCOEt; $n = 67$; $P = 0.5$, compared with vehicle, Mann–Whitney U test) and by the mGluR₅ antagonist 2-methyl-6-(phenylethynyl) pyridine (MPEP; 40 μM ; $n = 103$; $t_{1/2} = 191$ s for quinpirole with MPEP; $P = 0.1$, compared to vehicle, Mann–Whitney U test), while CPCCOEt ($t_{1/2} = 196$ s; $n = 99$; $P = 0.2$, compared to vehicle, Mann–Whitney U test) or MPEP ($t_{1/2} = 208$ s; $n = 71$; $P = 0.1$, compared to vehicle, Mann–Whitney U test) alone had no effect on FM1-43 release (Fig. 3G).

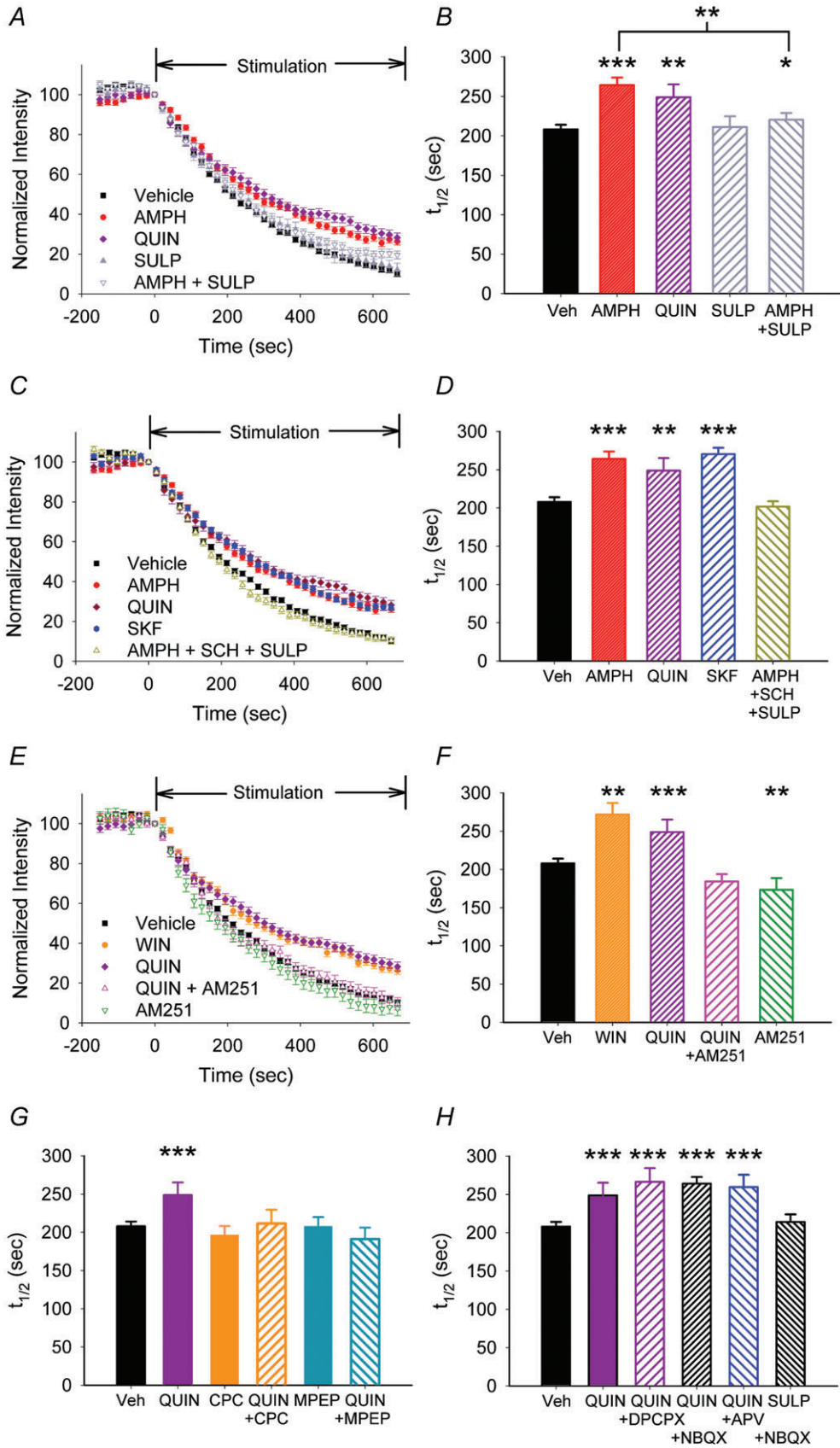
Unlike that found with the D1R agonist, inhibition by D2Rs was not mediated through A₁ adenosine, NMDA or AMPA receptors since quinpirole combined with their respective antagonists, DPCPX, ($t_{1/2} = 266$ s; $n = 68$; $P = 0.4$, compared with quinpirole, Mann–Whitney U test), NBQX ($t_{1/2} = 264$ s; $n = 221$; $P = 0.3$, compared with quinpirole, Mann–Whitney U test) and APV ($t_{1/2} = 259$ s; $n = 75$; $P = 0.4$, compared with quinpirole, Mann–Whitney U test), had no effect on the presynaptic release (Fig. 3H). Similarly, NBQX did not modify release following treatment with the D2R antagonist sulpiride ($t_{1/2} = 214$ s for NBQX with sulpiride, $n = 137$ vs. 206 s for NBQX alone; $P = 0.5$, Mann–Whitney U test) (Fig. 3H). The results indicate that endocannabinoids generate a strong regulatory effect on presynaptic excitation following high frequency stimulation; their actions are facilitated through D2R and group 1 mGluRs and are independent of A₁ adenosine, AMPA, NMDA and D1 receptors.

D1Rs enhance corticoaccumbal release when glutamate receptors are blocked

To eliminate all glutamate-activated retrograde pathways that might produce presynaptic modulation, we exposed striatal slices to the AMPAR antagonist

Figure 2. D1R-mediated inhibition of corticoaccumbal release requires adenosine

A, FM1-43 destaining curves show that, compared to vehicle (Veh), amphetamine or the D1R agonist SKF38393 reduced corticoaccumbal release. The D1R antagonist SCH23390 (SCH) had no effect on release and only partially blocked inhibition by amphetamine (AMPH+SCH). B, distribution of the mean $t_{1/2}$ of release for the destaining curves shown in panel A. For all panels, * $P < 0.05$, ** $P < 0.01$, *** $P < 0.001$, Mann–Whitney U test. C, similar to SKF38393, adenosine (ADEN) inhibited FM1-43 release. DPCPX alone did not alter destaining but blocked the inhibition produced by SKF38393 (SKF + DPCPX). D, distribution of the mean $t_{1/2}$ of release for the destaining curves shown in panel C. E, the NMDAR antagonist APV prevented inhibition by SKF38393 (SKF + APV), while the CB₁R antagonist AM251 did not significantly alter FM1-43 destaining (SKF + AM251). F, distribution of the mean $t_{1/2}$ of release for the destaining curves shown in panel E. G, the AMPAR antagonist NBQX with or without SCH23390 did not alter destaining. However, NBQX diminished, but did not completely reverse, presynaptic inhibition produced by SKF38393 (SKF + NBQX). H, distribution of the mean $t_{1/2}$ of release for the destaining curves shown in panel G.



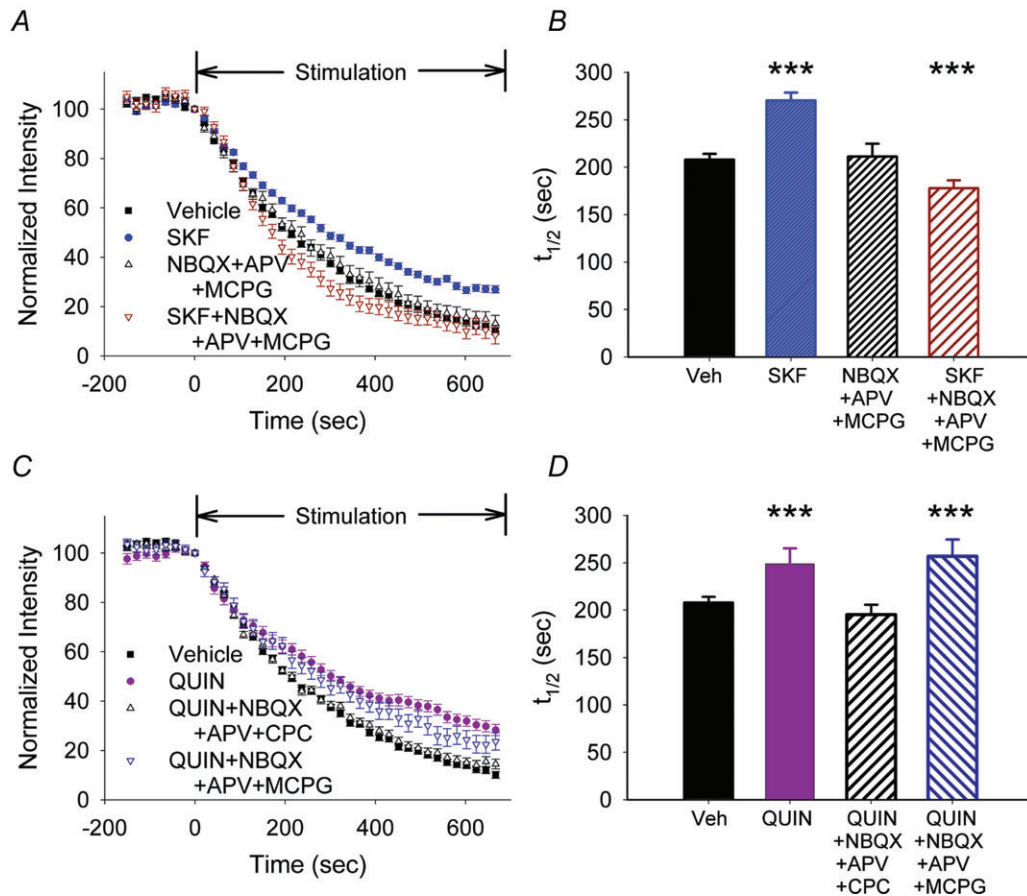


Figure 4. D1Rs boost corticoaccumbal release when glutamate receptors are blocked

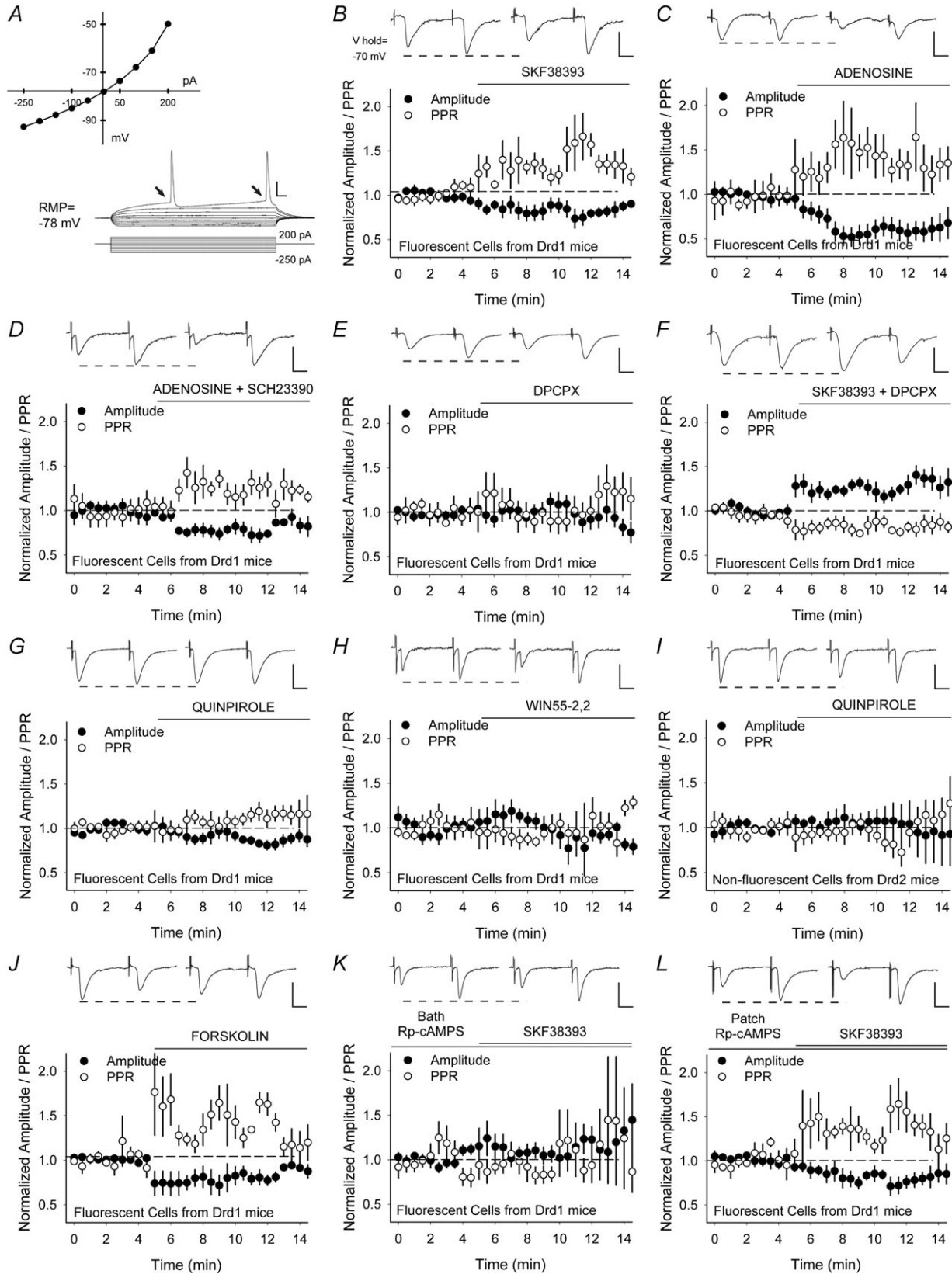
A, FM1-43 destaining curves showed that blockade of glutamate receptors with NBQX, APV and MCPG alone did not alter FM1-43 destaining but they blocked inhibition and further potentiated release when combined with SKF38393. **B**, average destaining half-times treatments shown in panel A. **C**, inhibition by the D2R agonist quinpirole was prevented by the glutamate antagonists NBQX, APV and CPCCOEt. The glutamate antagonists NBQX, APV and MCPG did not alter destaining after quinpirole. **D**, distribution of mean $t_{1/2}$ of release for destaining curves shown in panel C.

NBQX, the NMDAR antagonist APV, and the competitive antagonist at group 1 and 2 mGluRs, (+/-)- α -methyl-4-carboxyphenylglycine (MCPG; 300 μ M). This cocktail of glutamatergic receptor

antagonists alone did not alter corticoaccumbal release ($t_{1/2} = 210$ s for NBQX, APV and MCPG; $n = 107$ puncta; $P = 0.5$, compared to vehicle, Mann-Whitney U test) (Fig. 4A and B). However, in the presence of the D1R

Figure 3. D2Rs produce corticoaccumbal inhibition through endocannabinoids

A, FM1-43 destaining curves revealed that both amphetamine and quinpirole ($n = 80$) reduced corticoaccumbal release. Sulpiride (SULP) alone did not alter destaining and only partially blocked inhibition by amphetamine (AMPH + SULP). **B**, distribution of the mean $t_{1/2}$ of release for the destaining curves shown in panel A. For all panels, * $P < 0.05$, ** $P < 0.01$, *** $P < 0.001$, Mann-Whitney U test. **C**, compared to vehicle, amphetamine, quinpirole and SKF38393 reduced corticoaccumbal destaining. Only the combination of D1 and D2 receptor antagonists, SCH23390 and sulpiride, respectively, prevented inhibition by amphetamine (AMPH + SCH + SULP). **D**, distribution of the mean $t_{1/2}$ of release for destaining curves shown in panel C. **E**, the CB₁R agonist, WIN55-2,2 (WIN) decreased exocytosis to a similar extent as quinpirole, while AM251 blocked inhibition by quinpirole (QUIN + AM251). AM251 alone boosted FM1-43 destaining. **F**, distribution of the mean $t_{1/2}$ of release for the experiments shown in panel E. **G**, the mGluR₁ antagonist CPCCOEt (CPC) did not modify FM1-43 destaining but blocked inhibition by quinpirole (CPC + QUIN). Similarly, the mGluR₅ antagonist MPEP did not modify FM1-43 destaining and blocked inhibition by quinpirole (MPEP + QUIN). **H**, the A₁ adenosine, NMDA and AMPA receptor antagonists DPCPX, NBQX and APV, respectively, did not block inhibition by quinpirole. Sulpiride with NBQX (SULP + NBQX) did not change FM1-43 destaining.



agonist SKF38393, the cocktail blocked presynaptic inhibition and further accelerated release from terminals with a low probability of release (Supplementary Fig. S7) beyond that observed in untreated slices ($t_{1/2} = 177$ s for NBQX, APV and MCPG with SKF38393; $n = 92$; $P < 0.001$, compared to vehicle, Mann–Whitney U test) (Fig. 4A and B), thereby unmasking an excitatory D1R effect that boosted corticoaccumbal release.

Inhibition generated by the D2R agonist quinpirole was also prevented when the mGluR₁ antagonist CPCCOEt was combined with NBQX and APV ($t_{1/2} = 196$ s; $n = 68$; $P < 0.001$, compared to quinpirole alone, Mann–Whitney U test), but these combined antagonists did not potentiate FM1-43 exocytosis ($P = 0.2$, compared to vehicle, Mann–Whitney U test) (Fig. 4C and D). The non-selective mGluR antagonist MCPG along with NBQX and APV failed to alter presynaptic inhibition by quinpirole ($t_{1/2} = 256$ s for quinpirole with MCPG, NBQX and APV; $n = 126$; $P = 0.5$, compared to quinpirole, Mann–Whitney U test) (Fig. 4C and D), further indicating that control over endocannabinoid efflux was restricted to group 1 mGluRs.

Whole cell electrophysiology experiments show that D1 and A₁ receptors differentially regulate glutamate release onto striatonigral neurons

While optical recordings provided a measure of activity-dependent release from presynaptic terminals, they were not sensitive to those terminals synapsing on subtypes of MSNs. Thus, electrophysiological recordings were obtained in fluorescent and non-fluorescent MSNs from hemizygotic *Drd1*- and *Drd2*-EGFP mice to detect alterations in glutamate release from terminals specifically innervating D1 (D1R+) and D2 (D2R+) receptor-expressing MSNs. Evoked (e) EPSCs in fluorescent MSNs from *Drd1*-EGFP mice (Fig. 5A) were measured in response to PFC stimulation with 20 Hz paired-pulses delivered every 30 s (Fig. 1B). The D1R

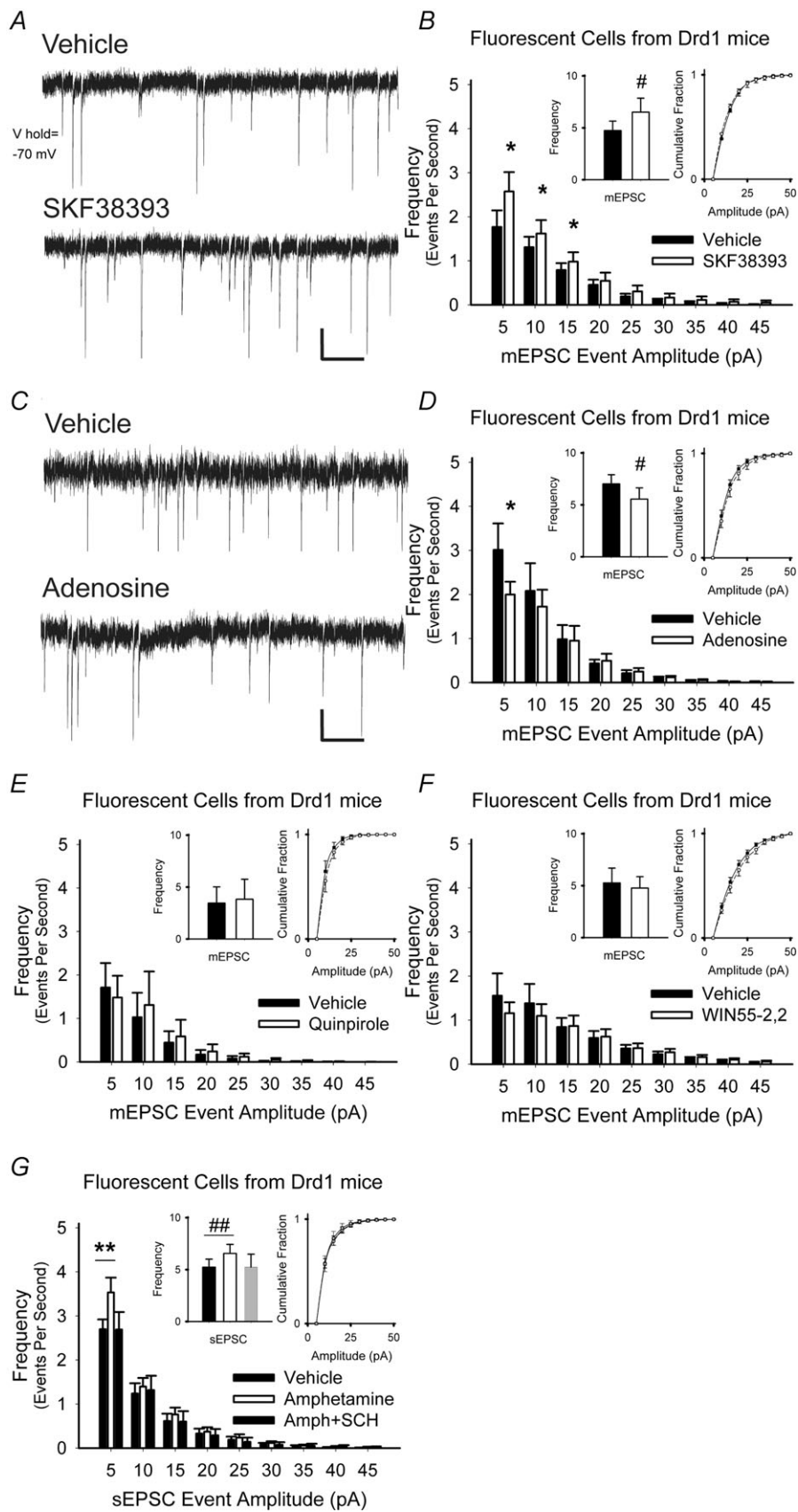
agonist SKF38393 decreased the amplitude of the first current of the pair by $16 \pm 7\%$ (-103 ± 24 pA for vehicle *vs.* -89 ± 18 pA following SKF38393; $n = 7$ cells; $P = 0.04$, Student's paired t test) and increased the paired-pulse ratio (PPR; amplitude of the second eEPSC/amplitude of the first eEPSC) by $45 \pm 13\%$ (1.15 ± 0.18 in vehicle to 1.62 ± 0.24 in SKF38393; $P = 0.02$, Student's paired t test) (Fig. 5B), indicating a reduction in corticoaccumbal excitation.

Adenosine also reduced presynaptic activity since the amplitude of the first current of the pair by decreased by $41 \pm 10\%$ (-79 ± 17 pA for vehicle *vs.* -38 ± 7 pA following adenosine; $n = 8$; $P = 0.04$, Student's paired t test) and the PPR increased by $46 \pm 13\%$ (0.93 ± 0.08 in vehicle *vs.* 1.34 ± 0.22 in adenosine; $P = 0.02$, Student's paired t test) (Fig. 5C). Adenosine was sufficient to produce presynaptic inhibition, since it remained inhibitory in the presence of the D1R antagonist SCH23390; the amplitude of the first current of the pair decreased by $34 \pm 11\%$ (-52 ± 8 pA for vehicle *vs.* -33 ± 8 pA following SCH23390 and adenosine; $n = 5$; $P = 0.02$, Student's paired t test) and the PPR increased by $15 \pm 4\%$ (1.33 ± 0.17 in vehicle *vs.* 1.58 ± 0.32 in SCH23390 and adenosine; $P = 0.03$, Student's paired t test) (Fig. 5D).

The A₁ adenosine receptor antagonist DPCPX alone had no effect on either the amplitude ($-1 \pm 8\%$; -76 ± 27 pA for vehicle *vs.* -73 ± 24 pA with DPCPX; $n = 7$; $P = 0.6$, Student's paired t test) or the PPR ($13 \pm 13\%$; 1.21 ± 0.11 in vehicle *vs.* 1.32 ± 0.14 in DPCPX; $P = 0.4$, Student's paired t test) (Fig. 5E), indicating a lack of tonic inhibition by adenosine. However, when DPCPX was combined with the D1R agonist, the amplitude of the first eEPSC increased by $18 \pm 6\%$ (-81 ± 12 pA for vehicle *vs.* -96 ± 16 pA for SKF38393 with DPCPX; $n = 10$; $P = 0.03$, Student's paired t test) and the PPR decreased by $13 \pm 3\%$ (1.37 ± 0.14 in vehicle *vs.* 1.19 ± 0.18 in SKF38393 and DPCPX; $P = 0.007$, Student's paired t test) (Fig. 5F), indicating presynaptic excitation through D1Rs in the absence of A₁R stimulation.

Figure 5. Recordings in fluorescent MSNs from *Drd1*-EGFP mice show that presynaptic inhibition by D1Rs is dependent on adenosine, adenylyl cyclase and PKA

A, the current–voltage plot generated by depolarizing current pulses shows inward rectification (arrows) and regular firing behaviour, typical for MSNs. B, representative traces show the average responses of paired-pulses before (above, left) and 5 to 7.5 min following bath application of SKF38393 (above, right). Graph shows the normalized amplitude of the first eEPSC (of the pair) and the normalized PPR. SKF38393 and C, adenosine decreased the amplitude of the first eEPSC and increased the PPR. D, adenosine combined with the D1R antagonist SCH23390 decreased the amplitude of the first eEPSC and increased the PPR. E, the A₁ adenosine antagonist DPCPX had no effect on the eEPSC amplitude or PPR. F, in the presence of DPCPX, SKF38393 increased the eEPSC amplitude and decreased the PPR. G, the D2R agonist quinpirole and H, the CB₁R agonist WIN55-2,2 had no effect on the eEPSC amplitude or the PPR. I, in non-fluorescent cells from *Drd2*-EGFP mice, quinpirole had no effect on the eEPSC amplitude or the PPR. J, forskolin reduced the eEPSC amplitude in fluorescent cells from *Drd1*-EGFP mice and increased the PPR. K, bath application of the PKA inhibitor Rp-cAMPS blocked inhibition by SKF38393. L, when Rp-cAMPS was applied via the patch electrode, SKF38393 remained inhibitory, as the eEPSC amplitude decreased and the PPR increased. Bar in A: 10 mV, 25 ms. Bar in B–L: 100 pA, 12.5 ms.



D2 and CB₁ receptors did not modulate eEPSCs in D1R+ neurons, as the D2R agonist quinpirole (5 μ M) did not change the eEPSC amplitude ($-12 \pm 7\%$; -197 ± 31 pA for vehicle *vs.* -168 ± 33 pA following quinpirole; $n = 6$; $P = 0.1$, Student's paired *t* test) or the PPR ($5 \pm 7\%$; 1.01 ± 0.16 in vehicle to 1.13 ± 0.18 in quinpirole; $P = 0.1$, Student's paired *t* test) (Fig. 5G) and the CB₁R agonist WIN55-2,2 had no effect on the eEPSC amplitude ($-19 \pm 11\%$; -130 ± 49 pA for vehicle *vs.* -119 ± 52 pA following WIN55-2,2; $n = 6$; $P = 0.5$, Student's paired *t* test) or the PPR ($18 \pm 13\%$; 1.38 ± 0.24 in vehicle to 1.65 ± 0.36 in WIN55-2,2; $P = 0.2$, Student's paired *t* test) (Fig. 5H). Likewise, quinpirole did not change the eEPSC amplitude ($2 \pm 15\%$; -74 ± 7 pA in vehicle *vs.* -75 ± 13 pA in quinpirole; $n = 7$; $P = 0.5$, Student's paired *t* test) or the PPR ($-10 \pm 9\%$; 1.38 ± 0.19 in vehicle *vs.* 1.3 ± 0.24 in quinpirole; $P = 0.4$, Student's paired *t* test) in non-fluorescent cells from Drd2-EGFP mice (Fig. 5I).

Inhibition by adenosine requires activation of adenylyl cyclase and protein kinase A (PKA) in striatonigral MSNs

Activation of adenylyl cyclase, cAMP and PKA are required for signalling by Gs-protein coupled receptors (Memo *et al.* 1986) and adenosine production in the hippocampus (Brundege *et al.* 1997; Dunwiddie & Masino, 2001). Similar to the D1R agonist, bath application of forskolin (FSK; 10 μ M), a potent membrane-permeant activator of adenylyl cyclase (Laurenza *et al.* 1989), briskly reduced the eEPSC amplitude in D1R-expressing cells by $15 \pm 5\%$ (-75 ± 22 pA for vehicle *vs.* -63 ± 16 pA following forskolin; $n = 6$ cells; $P = 0.04$, Student's paired *t* test) and increased the PPR by $35 \pm 6\%$ (1.07 ± 0.15 in vehicle *vs.* 1.39 ± 0.29 in forskolin; $P = 0.02$, Student's paired *t* test) (Fig. 5J). When the membrane-permeant PKA inhibitor Rp-cAMPS (10 μ M) was bath applied, SKF38393 had no effect on corticoaccumbal activity; there was no change in the eEPSC amplitude ($4 \pm 12\%$;

-67 ± 7 pA for Rp-cAMPS *vs.* -74 ± 12 pA following SKF38393 with Rp-cAMPS; $n = 7$; $P = 0.5$, Student's paired *t* test) or in the PPR ($-13 \pm 20\%$; 1.51 ± 0.35 in Rp-cAMPS *vs.* 1.36 ± 0.17 in SKF38393 and Rp-cAMPS; $P = 0.6$, Student's paired *t* test) (Fig. 5K). These results suggest that forskolin and SKF38393 modulated corticoaccumbal activity through adenylyl cyclase and PKA.

To confirm that presynaptic mechanisms were involved, we made recordings with internal solutions containing 400 μ M Rp-cAMPS (Ding *et al.* 2003). When Rp-cAMPS was applied via the patch electrode, SKF38393 remained inhibitory; the eEPSC amplitude decreased by $28 \pm 9\%$ (-71 ± 10 pA for vehicle *vs.* -58 ± 13 pA following SKF38393; $n = 7$; $P = 0.02$, Student's paired *t* test) and the PPR increased ($23 \pm 6\%$; 1.28 ± 0.17 in vehicle to 1.74 ± 0.37 *vs.* SKF38393; $P = 0.04$, Student's paired *t* test) (Fig. 5L), suggesting that the presynaptic depression caused by SKF38393 did not arise through mechanisms intrinsic to the neuron under evaluation.

D1Rs excite while A₁Rs inhibit presynaptic activity of striatonigral neurons

To further localize D1 and A₁ receptors on cortical afferents of fluorescent MSNs in Drd1-EGFP mice, miniature (m) EPSCs were observed in the presence of the Na⁺ channel antagonist TTX, which blocked spontaneous cortically derived action potentials and isolated activity at the presynaptic terminal. The D1R agonist SKF38393 increased the frequency of mEPSC by $35 \pm 16\%$ (4.77 ± 0.91 Hz in vehicle *vs.* 6.51 ± 1.34 Hz in SKF38393; $n = 9$; $P = 0.04$, Student's paired *t* test), by selectively increasing high-frequency, low-amplitude inward currents (Fig. 6A and B). There was no difference in the distribution of mEPSC amplitudes (Fig. 6B), indicating that the increase in mEPSCs frequency was likely to be attributable to the potentiating effect of SKF38393 on presynaptic release (Van der Kloot, 1991). Conversely, adenosine diminished the frequency of mEPSC in D1R-presenting MSNs by $21 \pm 6\%$ (7.02 ± 0.88 Hz in vehicle *vs.* 5.55 ± 1.09 Hz

Figure 6. D1 and A₁ adenosine receptors modulate presynaptic activity in fluorescent cells from Drd1-EGFP mice

A, representative mEPSCs in D1R+ cells (upper trace) increased 5 min after exposure to the D1R agonist SKF38393 (lower trace). B, SKF38393 increased the frequency of mEPSCs (inset, left) by boosting the number of high-frequency, low-amplitude spontaneous inward currents while having no effect on the cumulative distributions of mEPSC amplitudes (inset, right). For panels B and D–G, * $P < 0.05$, ** $P < 0.01$, Student's *t* test with Bonferroni adjustment and # $P < 0.05$, ## $P < 0.01$, Student's paired *t* test. C, representative mEPSCs in D1R+ cells (upper trace), decreased after exposure to adenosine (lower trace). D, adenosine reduced the frequency of low-amplitude mEPSCs but had no effect on the distribution of mEPSC amplitudes. E, the D2R agonist quinpirole did not alter the frequency, the frequency distribution or the amplitude distribution of mEPSCs in D1R+ cells. F, the CB₁R agonist WIN55-2,2 also had no effect on the mEPSC frequency, the frequency distribution or the amplitude distribution in D1R-expressing cells. G, amphetamine increased in frequency, but not amplitude distribution, of sEPSCs D1R+ cells. Excitation by amphetamine was blocked by the D1R antagonist SCH23390 (SCH). Bar in panels A and C, 5 pA, 0.5 s.

in adenosine; $n = 7$; $P = 0.03$, Student's paired t test), by inhibiting high-frequency, low-amplitude events (Fig. 6C–D). Neither the D2R agonist quinpirole ($3.9 \pm 5\%$; 3.45 ± 1.56 Hz in vehicle vs. 3.82 ± 1.93 Hz in quinpirole; $n = 6$; $P = 0.4$, Student's paired t test) nor the CB₁R agonist WIN55-2,2 ($-0.8 \pm 9\%$; 5.26 ± 1.42 Hz in vehicle vs. 4.77 ± 1.09 Hz in WIN55-2,2; $n = 8$; $P = 0.4$, Student's paired t test) changed the frequency or amplitude distribution of mEPSCs (Fig. 6E–F). Thus, in the absence of stimulation, D1 receptors enhanced and A₁ adenosine receptors diminished the excitability of D1R-expressing cells at presynaptic terminals, while D2 and CB₁ receptors had no effect.

To determine the effect of amphetamine on cortico-accumbal neurotransmission under more physiological conditions, spontaneous (s) EPSCs (without TTX) were observed in D1R+ MSNs. These spontaneous synaptic currents probably represent release of individual transmitter quanta if there is no change in their amplitude distributions (Mennerick & Zorumski, 1995). Amphetamine increased the frequency, but not amplitude distribution of sEPSCs in all cells tested by $29 \pm 10\%$ (5.23 ± 0.78 Hz in vehicle vs. 6.56 ± 0.87 Hz in amphetamine; $n = 10$; $P = 0.01$, Student's paired t test). The increase in sEPSC frequency by amphetamine was prevented by the D1R antagonist SCH23390 (Fig. 6G), but not by the A₁ adenosine antagonist DPCPX (not shown; $P = 0.8$, Student's paired t test).

Synaptic activity promotes inhibition through adenosine and overrides excitation caused by D1Rs

To support these data, we also observed frequencies of mEPSC (with TTX) in MSNs from non-genetically manipulated WT mice. The D1R agonist SKF38393 increased the frequency of mEPSCs in all cells tested by $43 \pm 12\%$ (3.03 ± 0.89 Hz in vehicle vs. 3.98 ± 0.98 Hz in SKF38393; $n = 7$; $P = 0.01$, Student's paired t test) by increasing high-frequency events in the 5–15 pA range, but did not change the distribution of mEPSC amplitudes (Fig. 7A and F), indicating that D1Rs had a potentiating effect on presynaptic release.

Next, we used synaptic conditioning to confirm that inhibition produced though adenosine might override excitation caused by D1Rs. sEPSCs were observed in WT MSNs before and following conditioning stimuli, consisting of cortically applied paired-pulses at 20 Hz (Fig. 7B). In the absence of conditioning stimuli, the D1R agonist SKF38393 was excitatory ($70 \pm 15\%$; 1.35 ± 0.49 Hz in vehicle vs. 2.45 ± 0.9 Hz in SKF38393; $n = 8$; $P = 0.03$, Student's paired t test), and there was no change in the sEPSC amplitude distribution (Fig. 7C and F). Following conditioning stimuli, excitation by the D1R agonist was blocked and the frequency of sEPSCs declined

by $7 \pm 4\%$ (4.53 ± 0.54 Hz in vehicle vs. 4.06 ± 0.44 Hz in SKF38393; $n = 25$; $P = 0.03$, Student's paired t test), primarily by decreasing the frequency of spontaneous events in the 5–10 pA range (Fig. 7D and F). When adenosine A₁Rs were blocked, presynaptic depression was prevented and the frequency of sEPSCs increased by $23 \pm 3\%$ (8.78 ± 1.87 Hz in DPCPX vs. 10.65 ± 1.19 Hz in DPCPX combined with SKF38393; $n = 6$; $P < 0.001$, Student's paired t test), with a boost in 5–15 pA events (Fig. 7E and F). Thus, high frequency synaptic activity prevented excitation by the D1R and promoted presynaptic inhibition through A₁Rs.

CB₁ and D1 receptors differentially regulate glutamate release onto striatopallidal neurons

We first examined modulation of presynaptic activity to D2R+ MSNs using electrophysiological recordings in non-fluorescing cells from hemizygotic *Drd1*-EGFP mice, as the majority of these cells are likely to express D2Rs (Shuen *et al.* 2008). In these cells, quinpirole reduced the peak amplitude of the first eEPSC by $23 \pm 6\%$ (-164 ± 36 pA in vehicle vs. -126 ± 32 pA in quinpirole; $n = 6$ cells; $P = 0.05$, Student's paired t test) and the PPR increased by $9 \pm 2\%$ (1.01 ± 0.07 in vehicle vs. 1.1 ± 0.17 in quinpirole; $P = 0.02$, Student's paired t test) (Fig. 8A). Interestingly, compared to the rapid inhibition achieved by SKF38393 in D1R+ MSNs (Fig. 5B), the onset of presynaptic inhibition caused by quinpirole appeared relatively delayed (Fig. 8B).

Inhibition by D2Rs was dependent on endocannabinoids, since the CB₁R antagonist AM251 blocked inhibition by the D2R agonist; the amplitude of the first eEPSC ($-2 \pm 14\%$; -114 ± 27 pA for vehicle vs. -118 ± 29 pA for quinpirole with AM251; $n = 9$; $P = 0.8$, Student's paired t test) and the PPR ($-12 \pm 10\%$; 1.45 ± 0.21 in vehicle vs. 1.32 ± 0.21 in quinpirole with AM251; $P = 0.3$, Student's paired t test) remained unaffected (Fig. 8C). Further, in MSNs from CB₁^{+/+} mice, quinpirole reduced the eEPSC amplitude ($-18 \pm 7\%$; -91 ± 18 pA in vehicle vs. -80 ± 21 pA in quinpirole; $n = 7$; $P = 0.5$, Student's paired t test) and increased the PPR ($35 \pm 5\%$; 1.04 ± 0.11 in vehicle vs. 1.4 ± 0.21 in quinpirole; $P = 0.4$, Student's paired t test) (Fig. 8D), but not in cells from CB₁^{-/-} mice, where the eEPSC amplitude ($-3 \pm 16\%$; -137 ± 24 pA in vehicle vs. -124 ± 29 pA in quinpirole; $n = 6$; $P = 0.7$, Student's paired t test) and the PPR ($6 \pm 16\%$; 1.34 ± 0.11 in vehicle vs. 1.41 ± 0.24 in quinpirole; $P = 0.8$, Student's paired t test) remained unchanged (Fig. 8E). In support of the optical experiments, which showed that endocannabinoids promote some on-going inhibition of corticostriatal release in the absence of dopamine, the PPR

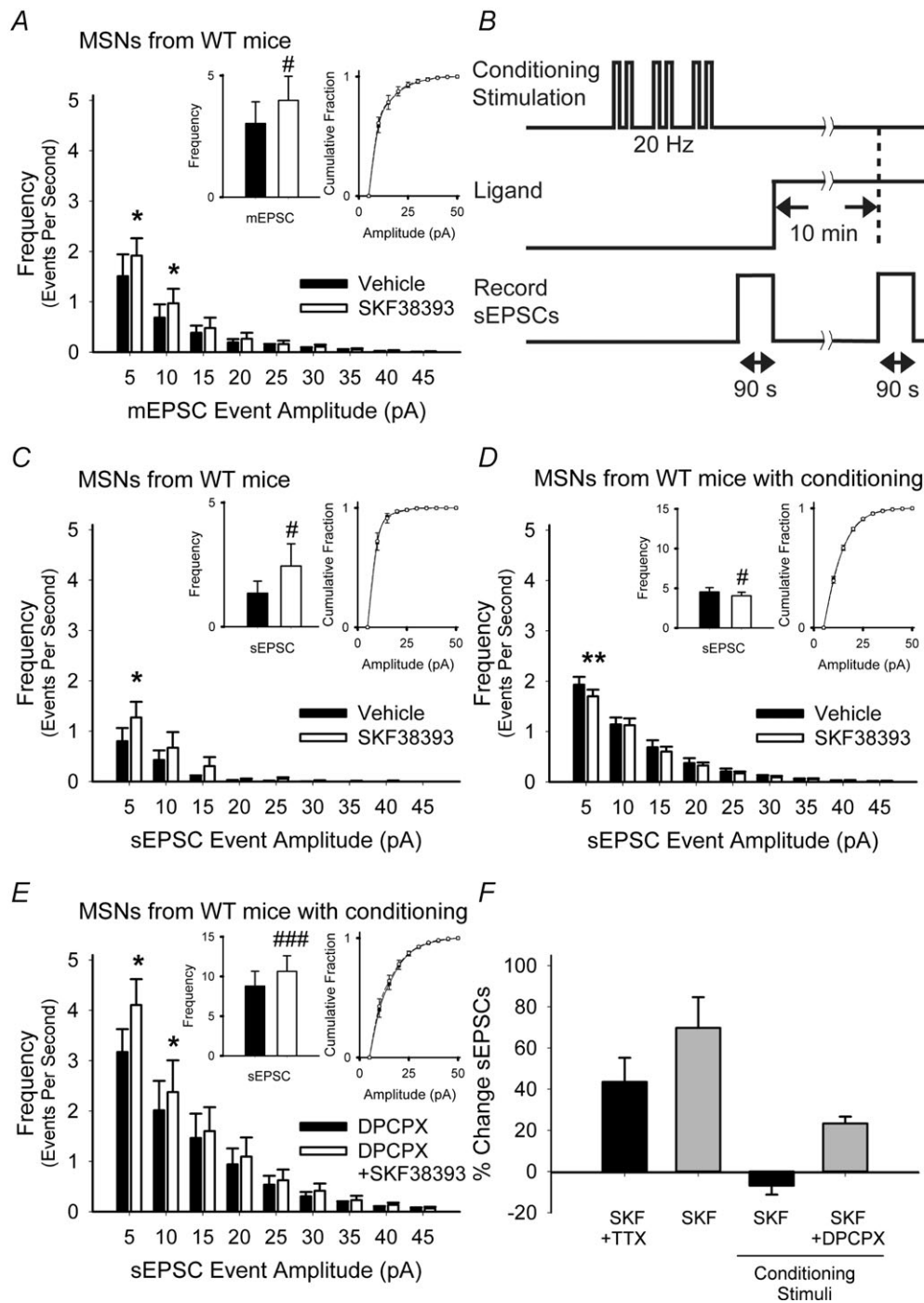


Figure 7. Synaptic activity in MSNs from WT mice prevents D1R-dependent presynaptic excitation and promotes inhibition through adenosine

A, SKF38393 increased the average frequency of 5–10 pA and 10–15 pA inward currents and did not alter the mEPSC amplitude distribution. For panels A and C–E, * $P < 0.05$, ** $P < 0.01$, Student's t test with Bonferroni adjustment and # $P < 0.05$, ### $P < 0.001$, Student's paired t test. B, protocol for synaptic conditioning with cortical stimulation. C, in the absence of conditioning, SKF38393 increased the frequency of 5–10 pA sEPSCs, but had no effect on the cumulative amplitude distribution. D, after conditioning stimuli were applied, SKF38393 reduced the average number of sEPSCs in the 5–10 pA range, but had no effect on their amplitude distributions. E, when the adenosine receptor antagonist DPCPX was applied along with conditioning stimuli, SKF38393 increased the average number of sEPSCs with amplitudes of 5–10 pA and 10–15 pA but did not alter their cumulative amplitude distributions. F, summary of changes in mEPSCs and sEPSCs following SKF38393 with and without synaptic conditioning.

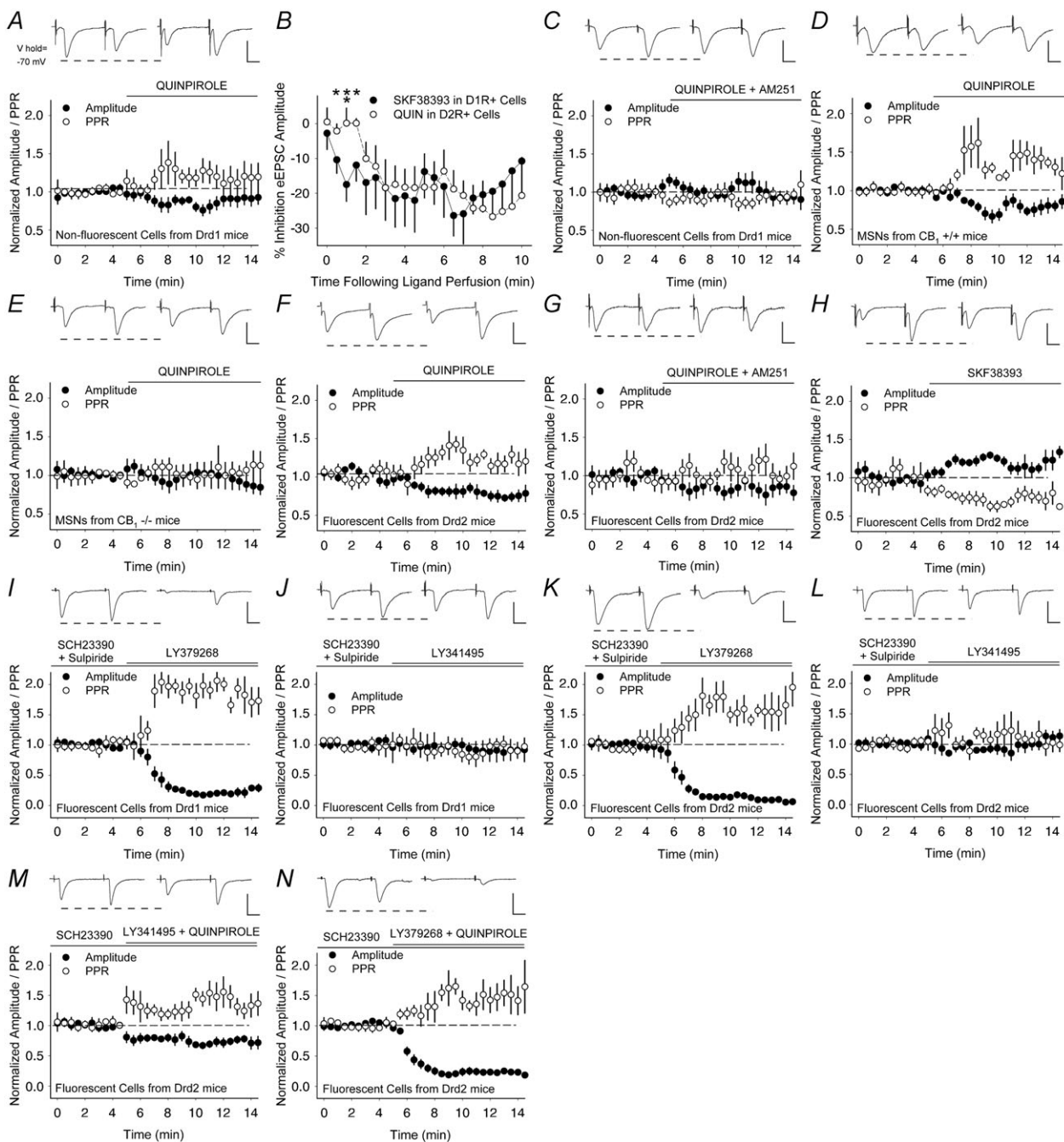


Figure 8. Presynaptic inhibition of D2R-expressing MSNs by D2Rs is prevented by endocannabinoids

A, the D2R agonist quinpirole decreased the amplitude of the first eEPSC (of the pair) and increased the PPR in non-fluorescent MSNs from Drd1-EGFP mice. B, inhibition of the eEPSC amplitude by quinpirole in D2R-expressing cells was delayed compared to inhibition by the D1R agonist SKF38393 in D1R-expressing cells. $*P < 0.05$, $**P < 0.01$, ANOVA. C, the CB₁R antagonist AM251 blocked inhibition by quinpirole in non-fluorescent cells from Drd1-EGFP mice. D and E, quinpirole decreased the amplitude and reduced the PPR in MSNs from CB₁^{+/+} mice (D), but not in cells from CB₁^{-/-} mice (E). F and G, in fluorescent cells from Drd2-EGFP mice, quinpirole decreased the eEPSC amplitude and increased the PPR (F) and AM251 prevented inhibition by quinpirole (G). H, the D1R agonist SKF38393 increased the eEPSC amplitude and reduced the PPR. I and J, in the presence of D1 and D2 receptor antagonists SCH23390 and sulpiride, the mGluR_{2/3} agonist LY379268 suppressed the amplitude and increased the PPR in D1R+ cells (I), while the mGluR_{2/3} antagonist had no effect (J). K and L, the mGluR_{2/3} agonist also suppressed the amplitude and increased the PPR in D2R+ cells (K), while the mGluR_{2/3} antagonist LY341495 had no effect (L). M and N, in the presence of the D1R antagonist SCH23390, the D2R agonist quinpirole remained inhibitory when combined with the mGluR_{2/3} antagonist (M), and the combination of mGluR_{2/3} agonist and quinpirole suppressed corticoaccumbal activity (N). Bar in panels A and C–N, 100 pA, 12.5 ms.

in MSNs from CB₁^{-/-} mice was significantly higher than in cells from CB₁^{+/+} mice ($P = 0.05$, ANOVA).

Because a substantial fraction of non-fluorescing MSNs might fail to detectably express the pathway-specific transgenes and thereby result in a mixed population of cells (Shuen *et al.* 2008), electrophysiological recordings were also obtained in fluorescent MSNs from Drd2-EGFP mice. In these cells, quinpirole also decreased the amplitude of eEPSCs by $26 \pm 8\%$ (-94 ± 26 pA in vehicle *vs.* -76 ± 23 pA in quinpirole; $n = 9$; $P = 0.03$, Student's paired *t* test) and increased the PPR by $7 \pm 2\%$ (1.38 ± 0.16 in vehicle *vs.* 1.48 ± 0.27 in quinpirole; $P = 0.003$, Student's paired *t* test) (Fig. 8F). The corticoaccumbal inhibition caused by quinpirole was blocked by the CB₁R antagonist, since the amplitude ($-10 \pm 9\%$; -62 ± 8 pA in vehicle *vs.* -52 ± 11 pA in quinpirole with AM251; $n = 8$; $P = 0.2$, Student's paired *t* test) and the PPR ($5 \pm 5\%$; 1.39 ± 0.15 in vehicle *vs.* 1.6 ± 0.33 in quinpirole with AM251; $P = 0.4$, Student's paired *t* test) remained unchanged (Fig. 8G).

D1Rs excited D2R+ cells, since the D1R agonist SKF38393 increased the eEPSC amplitude by $16 \pm 5\%$ (-81 ± 16 pA in vehicle *vs.* -96 ± 21 pA in SKF38393; $n = 6$; $P = 0.03$, Student's paired *t* test) and decreased the PPR by $32 \pm 10\%$ (1.41 ± 0.24 in vehicle *vs.* 1.1 ± 0.23 in SKF38393; $P = 0.01$, Student's paired *t* test) (Fig. 8H). Thus, while D1Rs excited D2R+ neurons, D2Rs promoted a much stronger inhibition at those same synapses through endocannabinoids. Since responses following quinpirole were similar between fluorescent cells obtained in Drd2-EGFP mice and non-fluorescent cells from Drd1-EGFP mice, any over-expression of D2R proteins in Drd2-EGFP mice (Kramer *et al.* 2011) did not significantly impact corticoaccumbal activity under these conditions.

Inhibition by D2Rs is independent of group 2 mGluRs

We tested whether group 2 mGluRs (mGluR_{2/3}) on cortical terminals (Testa *et al.* 1998) might modulate corticostriatal activity. For these experiments, the D1 and D2 receptor antagonists SCH23390 and sulpiride, respectively, were also added to the bath, since the mGluR_{2/3} can negatively regulate dopamine release and their antagonists can increase synaptic dopamine (Karasawa *et al.* 2010). Consistent with prior studies (Lovinger & McCool, 1995), the mGluR_{2/3} agonist LY379268 ((1S,2R,5R,6R)-2-amino-4-oxabicyclo[3.1.0]hexane-2,6-dicarboxylic acid; $1 \mu\text{M}$) strongly suppressed presynaptic activity in D1R+ MSNs since the eEPSC amplitude decreased by $-81 \pm 2\%$ (-193 ± 35 pA *vs.* -39 ± 10 pA in LY379268; $n = 5$; $P = 0.004$, Student's paired *t* test) and the PPR increased by $78 \pm 24\%$ (0.94 ± 0.11 *vs.* 1.6 ± 0.33 in LY379268; $P = 0.02$, Student's paired *t* test) (Fig. 8I). There was no tonic inhibition by

mGluR_{2/3}, as the mGluR_{2/3} antagonist LY341495 (2-[(1S,2S)-2-carboxycyclopropyl]-3-(9H-xanthen-9-yl)-D-alanine; 100 nM) did not change the eEPSC amplitude ($-7 \pm 14\%$; -92 ± 21 pA *vs.* -94 ± 31 pA in LY341495; $n = 4$; $P = 0.9$, Student's paired *t* test) or the PPR ($-12 \pm 14\%$; 1.23 ± 0.2 *vs.* 1.02 ± 0.15 in LY341495; $P = 0.2$, Student's paired *t* test) (Fig. 8J).

The mGluR_{2/3} agonist also reduced corticostriatal activity in D2R+ cells since the eEPSC amplitude decreased by $85 \pm 4\%$ (-122 ± 20 pA *vs.* -20 ± 7 pA in LY379268; $n = 6$; $P = 0.005$, Student's paired *t* test) and the PPR increased by $26 \pm 6\%$ (1.19 ± 0.13 *vs.* 1.63 ± 0.32 in LY379268; $P = 0.02$, Student's paired *t* test) (Fig. 8K). Similar to D1R+ cells, the mGluR_{2/3} antagonist did not change the eEPSC amplitude ($-1 \pm 9\%$; -65 ± 15 pA *vs.* -64 ± 18 pA in LY341495; $n = 7$; $P = 0.9$, Student's paired *t* test) or the PPR ($-0.3 \pm 12\%$; 1.36 ± 0.16 *vs.* 1.33 ± 0.19 in LY341495; $P = 0.8$, Student's paired *t* test) (Fig. 8L).

Next, we determined whether mGluR_{2/3} might modulate D2R-dependent presynaptic inhibition in D2R+ MSNs. For these experiments, the D1R antagonist SCH23390 was added to the bath. Quinpirole remained inhibitory in the presence of the mGluR_{2/3} antagonist ($-32 \pm 6\%$; -70 ± 12 pA *vs.* -49 ± 12 pA in LY341495; $n = 7$; $P = 0.008$, Student's paired *t* test) and the PPR increased by $53 \pm 22\%$ (1.3 ± 0.12 *vs.* 1.97 ± 0.37 in LY341495; $P = 0.05$, Student's paired *t* test) (Fig. 8M). As expected, quinpirole in combination with the mGluR_{2/3} agonist LY379268 also strongly inhibited corticoaccumbal activity; the eEPSC amplitude decreased ($-75 \pm 6\%$; -206 ± 69 pA *vs.* -56 ± 19 pA in LY379268; $n = 5$; $P = 0.03$, Student's paired *t* test) and the PPR increased by $49 \pm 18\%$ (1.23 ± 0.15 *vs.* 1.88 ± 0.37 in LY379268; $P = 0.04$, Student's paired *t* test) (Fig. 8N). Thus, mGluR_{2/3} promoted strong presynaptic inhibition of both D1R+ and D2R+ cells, while presynaptic inhibition by D2Rs was independent of group 2 mGluRs.

D1Rs are excitatory, while both D2 and CB₁ receptors inhibit presynaptic activity of striatopallidal neurons

mEPSCs were recorded in fluorescent cells from Drd2-EGFP mice to further localize D1, A₁, D2 and CB₁ receptors on presynaptic terminals. The D1R agonist SKF38393 increased the frequency, but not the amplitude of mEPSC in fluorescent MSNs by $51 \pm 18\%$ (2.43 ± 0.65 Hz in vehicle *vs.* 3.12 ± 0.71 Hz in SKF38393; $n = 11$ cells; $P = 0.01$, Student's paired *t* test) by increasing high-frequency, low-amplitude events (Fig. 9A). Conversely, adenosine diminished the frequency of mEPSCs in D2R+ cells by $31 \pm 7\%$ (3.38 ± 0.78 Hz in vehicle *vs.* 2.03 ± 0.32 Hz with adenosine; $n = 10$; $P = 0.02$, Student's paired *t* test) while the amplitude distribution remained unchanged (Fig. 9B). Compared to

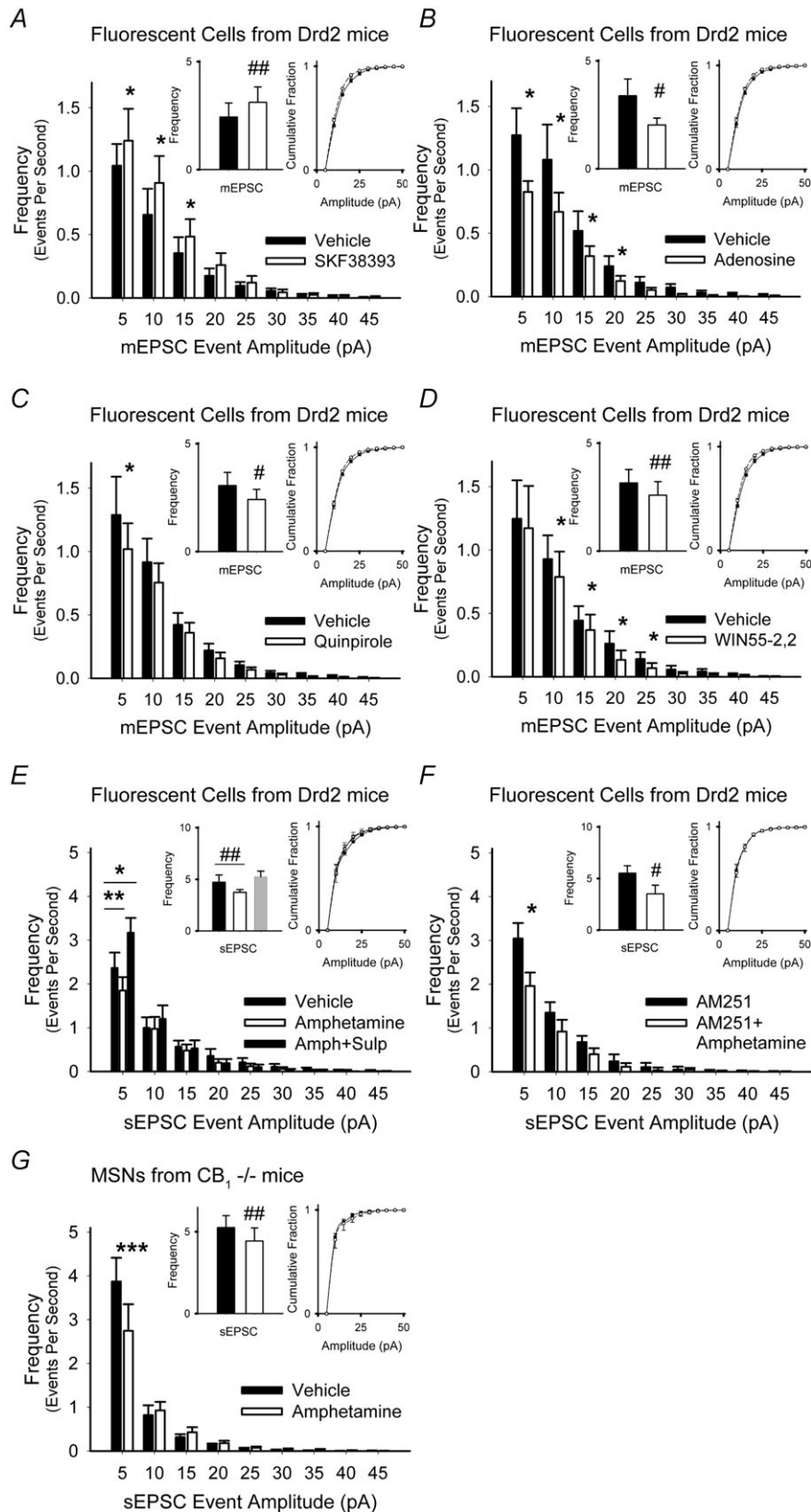


Figure 9. Excitatory D1Rs and inhibitory A₁, D2 and CB₁R_s modulate presynaptic inputs in Drd2-EGFP mice
A, the D1R agonist SKF38393 increased the frequency of mEPSCs by boosting the high-frequency, low-amplitude spontaneous inward currents but did not change the cumulative distribution of mEPSC amplitudes. For all panels, * $P < 0.05$, ** $P < 0.01$, *** $P < 0.001$, Student's t test with Bonferroni adjustment and # $P < 0.05$, ## $P < 0.01$, Student's paired t test. **B**, adenosine reduced the frequency of mEPSCs by broadly decreasing high-frequency, low-amplitude currents and did not change the mEPSC amplitude distribution. **C**, the D2R agonist quinpirole reduced the frequency of mEPSCs by specifically reducing high-frequency, low-amplitude inward currents but did not change the cumulative amplitude distribution. **D**, the CB₁R agonist WIN55-2,2 decreased mEPSC over a wide range of frequencies and did not change their amplitude distributions. **E**, amphetamine increased the frequency, but not the amplitude of sEPSCs in D2R+ cells. The D2R antagonist sulpiride blocked inhibition and the frequency of 5–10 pA inward currents increased. **F** and **G**, the frequency of sEPSCs was reduced by amphetamine with AM251 in D2+ cells (**F**), and also by amphetamine in MSNs from CB₁^{-/-} mice (**G**).

its selective inhibition of high-frequency, low-amplitude events in D1R+ cells, adenosine more broadly inhibited input frequencies to D2R+ MSNs (compare Figs 6D and 9B).

The D2R agonist quinpirole also reduced the frequency, but not the amplitude, of mEPSCs in D2R+ cells by $20 \pm 6\%$ (3.06 ± 0.61 Hz in vehicle *vs.* 2.41 ± 0.47 Hz with quinpirole; $n = 16$; $P = 0.04$, Student's paired *t* test) by depressing high-frequency, low-amplitude inward currents (Fig. 9C) and the CB₁R agonist WIN55-2,2 decreased the frequency, but not the amplitude distribution, in D2R+ cells by $22 \pm 7\%$ (3.15 ± 0.62 Hz in vehicle *vs.* 2.59 ± 0.63 Hz with WIN55-2,2; $n = 8$; $P = 0.01$, Student's paired *t* test) (Fig. 9D). Compared to quinpirole, WIN55-2,2 more broadly reduced mEPSC frequencies (compare Fig. 9C and D). Thus, D1Rs increased the frequency of mEPSCs, while D2 and CB₁ receptors were inhibitory.

We determined how dopamine might modulate corticoaccumbal inputs to D2R+ MSNs under more physiological conditions. Measurement of spontaneous inward currents in D2R+ cells indicated that amphetamine reduced the frequency, but not amplitude distribution, of sEPSCs by $23 \pm 13\%$ (4.71 ± 0.71 Hz in vehicle *vs.* 3.74 ± 0.67 Hz in amphetamine; $n = 7$; $P = 0.009$, Student's paired *t* test). This inhibition by amphetamine was produced by competition between D1 and D2 receptors, since the D2R antagonist sulpiride blocked the decrease in sEPSC frequency ($-0.5 \pm 8\%$; 5.25 ± 0.54 Hz; $P = 0.9$, compared to vehicle, Student's paired *t* test) and the frequency of 5–10 pA inward currents increased (Fig. 9E). Inhibition by quinpirole was at least partially independent of endocannabinoids since it persisted in the presence of the CB₁R antagonist AM251 ($-33 \pm 8\%$; 5.52 ± 0.71 Hz in vehicle *vs.* 3.51 ± 0.84 Hz in amphetamine; $n = 6$; $P = 0.03$, Student's paired *t* test) (Fig. 9F) and in CB₁^{-/-} mice ($-17 \pm 5\%$; 5.26 ± 0.73 Hz in vehicle *vs.* 4.44 ± 0.8 Hz in amphetamine; $n = 6$; $P = 0.01$, Student's paired *t* test) (Fig. 9G).

CB₁Rs inhibit presynaptic activity when synapses are active while D2Rs independently modulate glutamate release when synapses are quiet

To confirm these data, we also measured mEPSCs in non-genetically manipulated WT mice, where over-expression of D2Rs has not been found (Kramer *et al.* 2011). The frequency of mEPSC declined by $23 \pm 9\%$ in the D2R agonist (4.34 ± 0.73 Hz in vehicle *vs.* 3.5 ± 0.77 Hz in quinpirole; $n = 10$ cells; $P < 0.001$, Student's paired *t* test), primarily by reducing high-frequency, 5–10 pA events (Fig. 10A). Presynaptic inhibition by the D2R agonist was independent of CB₁Rs since quinpirole decreased mEPSCs in slices

from CB₁^{-/-} mice by $-13 \pm 2\%$ (2.94 ± 0.33 Hz in vehicle *vs.* 2.53 ± 0.43 Hz in quinpirole; $n = 12$; $P = 0.01$, Student's paired *t* test) and also in their CB₁^{+/+} littermates ($12 \pm 4\%$; 2.67 ± 0.31 Hz in vehicle *vs.* 2.38 ± 0.25 Hz in quinpirole; $n = 15$; $P = 0.007$, Student's paired *t* test) (Fig. 10B and C), suggesting that under non-stimulated conditions, D2Rs can also inhibit glutamate release in the absence of CB₁Rs. Tonic inhibition by endocannabinoids was lacking in the absence of evoked stimulation, since the frequency of mEPSC in MSNs from CB₁^{+/+} and CB₁^{-/-} mice were similar ($P = 0.44$, ANOVA).

To determine if synaptic activity might generate endocannabinoid inhibition at presynaptic terminals, sEPSCs (without TTX) were observed in MSNs from WT mice following conditioning stimuli, consisting of cortically applied paired-pulses at 20 Hz (Fig. 7B). When conditioning stimuli were applied, quinpirole depressed the frequency of sEPSCs ($-12 \pm 4\%$; 4.91 ± 0.66 Hz in vehicle *vs.* 4.22 ± 0.6 Hz in quinpirole; $n = 12$; $P = 0.01$, Student's paired *t* test) by inhibiting 5–10 pA inward currents (Fig. 10D). The CB₁R antagonist AM251 blocked the inhibition by quinpirole following conditioning stimuli (5.14 ± 0.52 Hz in AM251 *vs.* 5.26 ± 0.48 Hz in AM251 with quinpirole; $n = 15$; $P = 0.5$, Student's paired *t* test) (Fig. 10E) and no differences were observed in sEPSC amplitude distributions with or without AM251. These data suggest that presynaptic inhibition by endocannabinoids requires synaptic activity and that D2Rs may independently modulate glutamate release in their absence.

Discussion

Interactions between dopamine and glutamate in the NAc core are required for behavioural adaptations provoked by salient experiences (Pennartz *et al.* 1994) and these data show how dopamine can provide frequency-dependent and temporal modulation of corticoaccumbal activity in striatonigral and striatopallidal MSNs. At cortical frequencies below 10 Hz, presynaptic D1Rs excited both D1 and D2 receptor-expressing MSNs, while D2Rs specifically inhibited excitatory inputs to D2R-expressing cells. At higher cortical frequencies, dopamine promoted a prevailing inhibition of presynaptic corticoaccumbal terminals through adenosine and endocannabinoids, respectively. Adenosine production was dependent on activation of D1, AMPA and NMDA receptors and inhibited presynaptic activity to both D1 and D2R-expressing MSNs. Endocannabinoids caused a relatively late reduction in corticoaccumbal activity that specifically targeted D2R-expressing cells and was independent of AMPA, NMDA, group 2 mGlu, and D1 receptors, but required group 1 mGluRs. Thus, dopamine released following behavioural cues or psychostimulants

would increase corticoaccumbal excitation and promote strong signals along the striatonigral pathway while inhibiting the weak. Once activated, each population of D1 or D2 receptor-expressing output neuron could

curb their excitation through segregated retrograde pathways to encode signal patterns for striatal information processing (Geldwert *et al.* 2006; Mizuno *et al.* 2007) (Fig. 11).

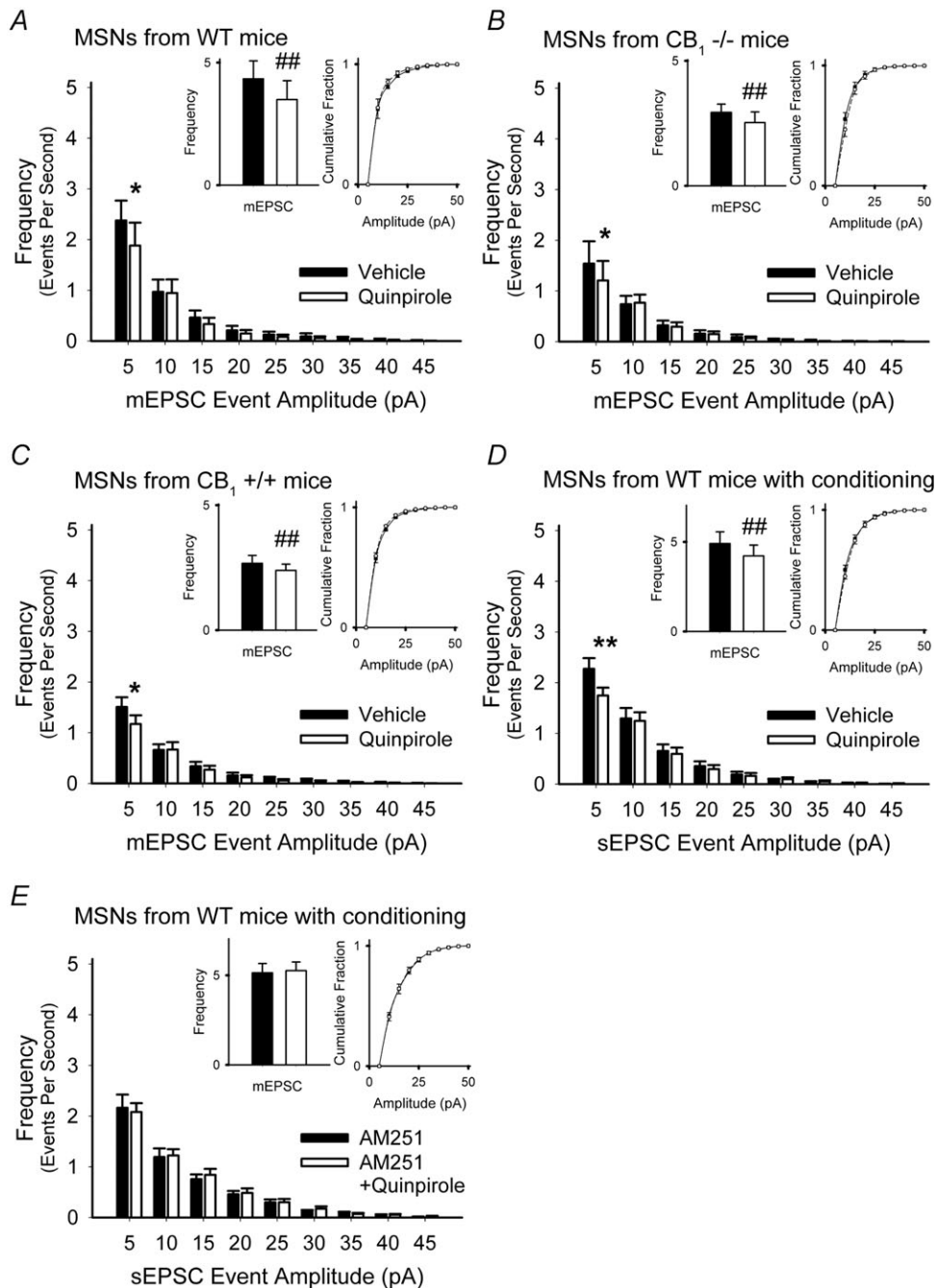


Figure 10. D2 and CB_1 receptors inhibit glutamate release in WT mice

A, the D2R agonist quinpirole decreased the average frequency of mEPSCs by reducing high-frequency, low-amplitude events but did not alter the cumulative mEPSC amplitude distribution. For all panels, $*P < 0.05$, $**P < 0.01$, Student's *t* test with Bonferroni adjustment and $###P < 0.001$, Student's paired *t* test. B and C, quinpirole reduced the frequency of mEPSCs in cells from $CB_1^{+/+}$ mice (B), and also in MSNs from $CB_1^{-/-}$ mice (C). D, quinpirole also reduced the frequency of sEPSCs in cells from WT mice following conditioning stimuli. E, after cortical conditioning stimuli were applied, the reduction in the frequency of sEPSCs by quinpirole was blocked by the CB_1 R antagonist AM251.

Results demonstrated how dopamine provides selective filtering at presynaptic corticoaccumbal terminals at low cortical frequencies. Unlike that found in the dorsal striatum (Maura *et al.* 1988; Hsu *et al.* 1995; Bamford *et al.* 2004*b*; Dumartin *et al.* 2007), we showed for the first time that D1Rs boosted glutamate release from terminals innervating both D1 and D2R-expressing MSNs with modulation likely occurring via presynaptic D1Rs located on ~25% of corticoaccumbal terminals (Dumartin *et al.* 2007). Under conditions of non-evoked, spontaneous glutamate release, amphetamine selectively and differentially modified the activity of high-frequency, low-amplitude excitatory currents to MSNs by producing a D1R-dependent excitation of D1R-expressing MSNs

while causing a net D2R-dependent reduction in the excitation of D2R-bearing cells. Although not sensitive to the type of MSN activated, the optical experiments revealed a similar pattern of excitation and inhibition from low-probability release terminals at cortical stimulation frequencies around 10 Hz, with amphetamine increasing exocytosis via D1Rs and decreasing exocytosis through D2Rs.

These opposing actions of D1 and D2 receptors on corticoaccumbal activity were occluded by the release of adenosine and endocannabinoids at higher cortical frequencies, which also dampened weak signals to D2 receptor-bearing MSNs and enhanced strong signals to D1R-expressing cells. Data suggest that when

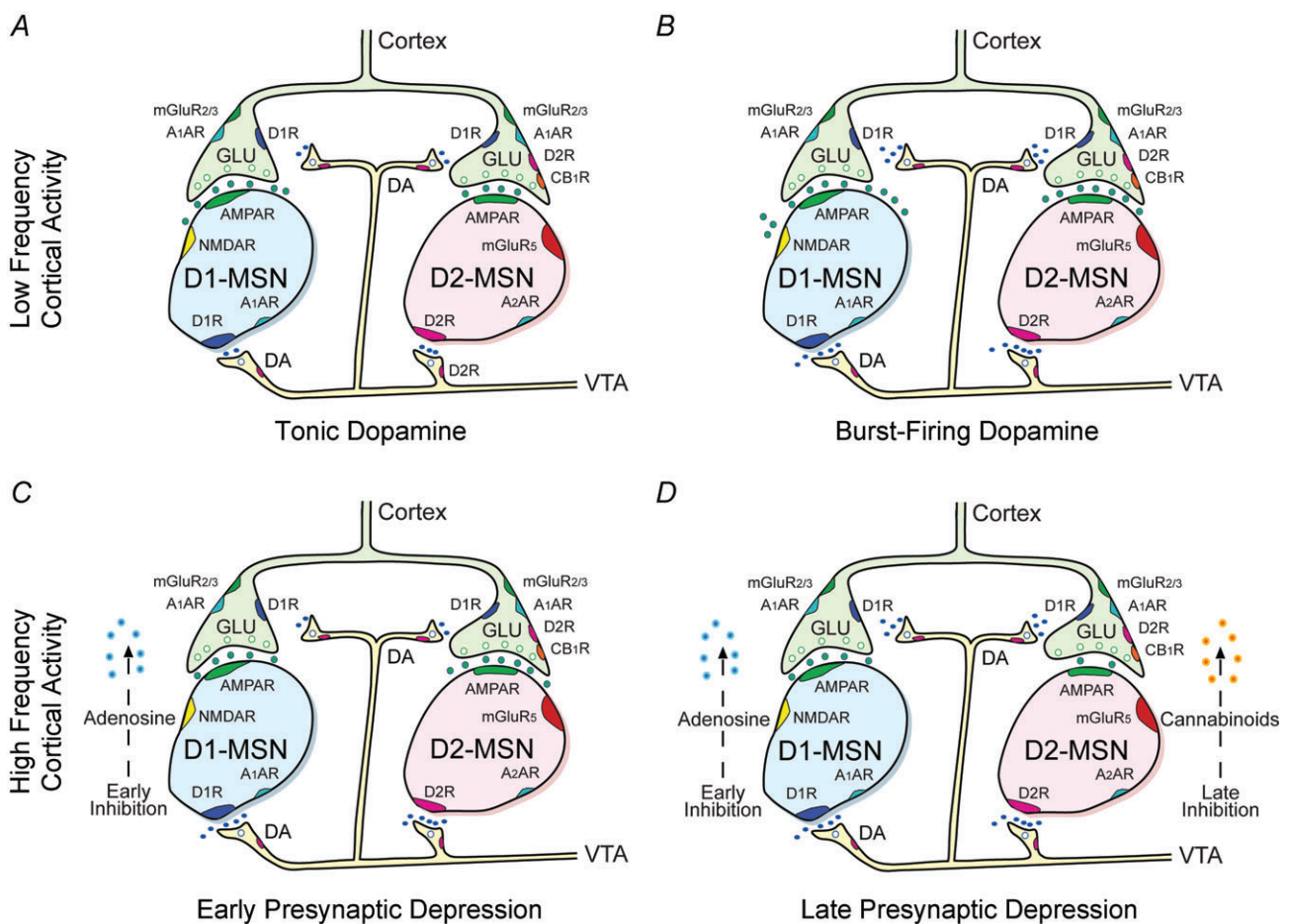


Figure 11. Proposed mechanism for signal processing by dopamine
 A, when corticoaccumbal neurons fire at low frequencies, tonic dopamine inhibits corticoaccumbal activity through D2Rs, which selectively inhibit low-release probability synapses on D2R-expressing MSNs. B, higher levels of evoked dopamine also modulate corticoaccumbal activity through D1Rs that strengthen glutamate release from presynaptic terminals innervating both D1 and D2R-expressing MSNs. C, when corticoaccumbal neurons fire a higher frequencies, dopamine promotes a much stronger modulation of presynaptic activity through adenosine. Adenosine inhibits presynaptic activity to both D1 and D2 receptor-expressing MSNs via A₁Rs and in D1-receptor expressing cells, is dependent on AMPA and NMDA receptor activation, as well as adenylate cyclase coupling in D1R-expressing MSNs. D, high frequency corticoaccumbal activity also promotes a selective presynaptic inhibition of D2R-expressing MSNs via CB₁Rs. Presynaptic inhibition by endocannabinoids is slower than adenosine, is strengthened by stimulation of D2Rs, and is dependent on group 1 mGlu receptors.

D1R-expressing striatal neurons were activated, postsynaptic D1Rs facilitated adenosine efflux and caused retrograde inhibition by decreasing the probability of glutamate release to D1 receptor-expressing MSNs. Stimulation of either D1 or A₁ receptors attenuated exocytosis from ~80% of cortical terminals, concordant with the percentage of adenosine receptors on striatal glutamatergic afferents (Ciruela *et al.* 2006) and selected strong synapses on D1-expressing MSNs while more broadly reducing synaptic transmission to D2R-bearing cells. Adenosine was sufficient to produce presynaptic inhibition in the absence of postsynaptic D1R activation and its actions at presynaptic terminals were augmented through G_{i/o} protein coupling by D1R- and forskolin-mediated stimulation of adenylyl cyclase and cAMP, which may then produce adenosine following dephosphorylation by ecto-nucleotidases (Dunwiddie & Masino, 2001). We also found that inhibition by adenosine was dependent on NMDAR stimulation and was potentiated by AMPARs, suggesting that D1 (Levine *et al.* 1996) and AMPA (Cherubini *et al.* 1988) receptors on MSNs may augment NMDAR-dependent calcium entry into postsynaptic cells (Huang *et al.* 2011) to promote adenosine production through signalling cascades (Husi *et al.* 2000; Hardingham *et al.* 2001) that are independent of adenylyl cyclase (Manzoni *et al.* 1994; Harvey & Lacey, 1997). These parallel mechanisms may share a common pathway (Dunwiddie & Masino, 2001) through cAMP (Sabatini *et al.* 2002; Vanhoutte & Bading, 2003; Dell'Acqua *et al.* 2006) since blockade of either adenylyl cyclase or NMDARs prevented inhibition triggered by the D1R agonist.

Activation of D2R-expressing striatal neurons at high cortical frequencies also encouraged further depression of the striatopallidal pathway through endocannabinoid signalling, which was strengthened at much higher cortical stimulation frequencies in the absence of amphetamine. D2Rs attenuated glutamate release by enhancing endocannabinoid efflux, presumably from MSNs (Di Marzo *et al.* 1994), after cortical stimulation was applied and more uniformly filtered cortical afferents to those same cells. Similar to that described in the dorsal striatum (Kreitzer & Malenka, 2005; Yin & Lovinger, 2006) and VTA (Pan *et al.* 2008), CB₁Rs had a strong modulatory effect on corticoaccumbal excitation that was driven by D2Rs following synaptic conditioning and was dependent on group 1, but not group 2, mGluRs. The D2R response was upstream from that of the mGluR and the CB₁ receptor, as blocking either receptor prevented the D2R agonist from inhibiting presynaptic release. These findings confirm and extend data in other studies showing that D2R-expressing MSNs specifically participate in activity-dependent reduction in the efficacy of neuronal synapses (Grueter *et al.* 2010) that can be expressed through presynaptic mechanisms (Choi &

Lovinger, 1997*a,b*). Both optical and electrophysiological recordings provided evidence of on-going inhibition by endocannabinoids at much higher stimulation frequencies in the absence of D2R activation. This supports existing evidence that cannabinoid-mediated presynaptic inhibition and LTD require some threshold level of synaptic activation that is provided at high cortical frequencies or following prolonged exposure to spontaneous activity (Adermark & Lovinger, 2007; Lovinger, 2010).

Interestingly, it appeared that a greater number of evoked synaptic currents were required to establish the full expression of endocannabinoid-mediated synaptic depression, as compared to the more rapid presynaptic attenuation caused by adenosine. This delay in endocannabinoid response is similar to that demonstrated during hippocampal LTD (Chevalyere & Castillo, 2003) and may be due to requisite glutamate efflux to extra-synaptic mGluRs (Yin & Lovinger, 2006). A failure or delay in generating a concentrated synaptic depression by endocannabinoids would lead to an imbalance in signals leaving the striatum via the striatonigral and striatopallidal projections, possibly affecting the viability of D2R-expressing MSNs, which may be susceptible to selective degeneration (Reiner *et al.* 1988; Joshi *et al.* 2009), and favour a shift from cannabinoid-induced LTD to long-term potentiation that develops through adenosine A_{2A} receptors on striatopallidal neurons (Higley & Sabatini, 2010).

We also found evidence for endocannabinoid-independent D2R inhibition at presynaptic afferents to striatopallidal pathway neurons. Under non-stimulated conditions, D2Rs inhibited spontaneous excitatory neurotransmission specific to D2R-expressing MSNs by reducing exocytosis from cortical terminals with a low probability of release. This depression of excitatory inward currents by D2Rs was in part independent of endocannabinoids, as it persisted in CB₁^{-/-} mice, and possibly occurred via D2Rs located on asymmetric, excitatory-type synapses in the NAc (Pickel *et al.* 2006), although contributions from other sources, including interneurons that also express D2Rs (Dawson *et al.* 1988; Seamans *et al.* 2001), are possible. Presynaptic D2Rs have been shown to facilitate cannabinoid-induced long-term depression (LTD) in the VTA (Pan *et al.* 2008) and may depress the probability of neurotransmitter release by inhibiting cAMP/PKA signalling at the presynaptic terminal (Neve *et al.* 2004; Howlett, 2005). Since inhibition by D2Rs was detected in CB₁^{-/-} mice in the absence of stimulation, dopamine may produce relatively weak synaptic filtering at low frequencies and provoke a more robust and overriding synaptic depression at higher frequencies by enhancing stimulus-dependent endocannabinoid efflux from MSNs, which can then bind to CB₁ or CB₁/D2 receptor heteromers on presynaptic terminals (Kearn

et al. 2005; Pickel *et al.* 2006; Marcellino *et al.* 2008).

Prior studies have generated apparently conflicting conclusions regarding the putative interactions between dopamine and glutamate within the NAc core. Results biased towards direct or indirect modulation, excitation or inhibition, or even a lack of response, might be attributed to the proportion of D1 and D2 receptor-expressing MSNs examined, by the presence or absence of synaptic stimulation, by differences in striatal anatomy or cortical stimulation frequency, or by the use of intra-striatal electrical stimulation to provoke synaptic activity that would likely release dopamine (Bamford *et al.* 2004b) and inadvertently modulate responses at the MSN.

It is tempting to speculate that selective filtering of low-probability synapses in the NAc core by dopamine, adenosine and endocannabinoids may be instrumental in determining the salience of sensory input and in defining the reinforcing properties associated with rewarding behaviour and attention (Pennartz *et al.* 1994). Pre-synaptic D1Rs that are selectively activated by dopamine burst firing in response to novel stimulation would initially lead to a stronger excitatory synaptic event but then, in an activity-dependent way, a subsequent lowering of the background at those same synapses via adenosine and endocannabinoids, thereby improving signal-to-noise while promoting attention on salient behavioural cues (Rebec, 1998; Dani & Zhou, 2004). These neuromodulators provide frequency-dependent filtering of excitatory inputs and also provide temporal filtering that leads to that selection. This activity-dependent filtering may accentuate particular synapses in space but also at a particular time. When different synapses are selected during motor learning, by the convergence of dopamine and cortical activity, oscillations between synaptic activation and depression may then enable sequencing of one motor task after another. Unwanted plasticity at striatal synapses due to alterations in dopamine, adenosine, endocannabinoid or glutamate availability or receptor sensitivity and expression would alter synaptic efficacy, promote an imbalance between striatonigral and striatopallidal pathways and contribute to symptoms and signs of neuropsychiatric disease.

References

- Adermark L & Lovinger DM (2007). Retrograde endocannabinoid signaling at striatal synapses requires a regulated postsynaptic release step. *Proc Natl Acad Sci U S A* **104**, 20564–20569.
- Albin RL, Young AB & Penney JB (1989). The functional anatomy of basal ganglia disorders. *Trends Neurosci* **12**, 366–375.
- Bamford NS & Cepeda C (2009). The corticostriatal pathway in parkinson's disease. In *Cortico-Subcortical Dynamics in Parkinson's Disease*, ed. Tseng KY, pp. 87–104. Humana Press, New York.
- Bamford NS, Robinson S, Palmiter RD, Joyce JA, Moore C & Meshul CK (2004a). Dopamine modulates release from corticostriatal terminals. *J Neurosci* **24**, 9541–9552.
- Bamford NS, Zhang H, Joyce JA, Scarlis CA, Hanan W, Wu NP, Andre VM, Cohen R, Cepeda C, Levine MS, Harleton E & Sulzer D (2008). Repeated exposure to methamphetamine causes long-lasting presynaptic corticostriatal depression that is renormalized with drug readministration. *Neuron* **58**, 89–103.
- Bamford NS, Zhang H, Schmitz Y, Wu NP, Cepeda C, Levine MS, Schmauss C, Zakharenko SS, Zablow L & Sulzer D (2004b). Heterosynaptic dopamine neurotransmission selects sets of corticostriatal terminals. *Neuron* **42**, 653–663.
- Brady AM & O'Donnell P (2004). Dopaminergic modulation of prefrontal cortical input to nucleus accumbens neurons in vivo. *J Neurosci* **24**, 1040–1049.
- Brundage JM, Diao L, Proctor WR & Dunwiddie TV (1997). The role of cyclic AMP as a precursor of extracellular adenosine in the rat hippocampus. *Neuropharmacology* **36**, 1201–1210.
- Cepeda C, Andre VM, Yamazaki I, Wu N, Kleiman-Weiner M & Levine MS (2008). Differential electrophysiological properties of dopamine D1 and D2 receptor-containing striatal medium-sized spiny neurons. *Eur J Neurosci* **27**, 671–682.
- Cepeda C, Bamford NS, Andre VM & Levine MS (2010). Alterations in corticostriatal synaptic function in Huntington's and Parkinson's diseases. In *Basal Ganglia Structure and Function*, ed. Steiner H & Tseng KY, pp. 607–623. Elsevier, San Diego.
- Cepeda C, Hurst RS, Altemus KL, Flores-Hernandez J, Calvert CR, Jokel ES, Grandy DK, Low MJ, Rubinstein M, Ariano MA & Levine MS (2001). Facilitated glutamatergic transmission in the striatum of D2 dopamine receptor-deficient mice. *J Neurophysiol* **85**, 659–670.
- Cherubini E, Herrling PL, Lanfumey L & Stanzione P (1988). Excitatory amino acids in synaptic excitation of rat striatal neurones *in vitro*. *J Physiol* **400**, 677–690.
- Chevalyere V & Castillo PE (2003). Heterosynaptic LTD of hippocampal GABAergic synapses: a novel role of endocannabinoids in regulating excitability. *Neuron* **38**, 461–472.
- Choi S & Lovinger DM (1997a). Decreased frequency but not amplitude of quantal synaptic responses associated with expression of corticostriatal long-term depression. *J Neurosci* **17**, 8613–8620.
- Choi S & Lovinger DM (1997b). Decreased probability of neurotransmitter release underlies striatal long-term depression and postnatal development of corticostriatal synapses. *Proc Natl Acad Sci U S A* **94**, 2665–2670.
- Ciruela F, Casado V, Rodrigues RJ, Lujan R, Burgueno J, Canals M, Borycz J, Rebola N, Goldberg SR, Mallol J, Cortes A, Canela EI, Lopez-Gimenez JF, Milligan G, Lluís C, Cunha RA, Ferre S & Franco R (2006). Presynaptic control of striatal glutamatergic neurotransmission by adenosine A1–A2A receptor heteromers. *J Neurosci* **26**, 2080–2087.

- Dani JA & Zhou FM (2004). Selective dopamine filter of glutamate striatal afferents. *Neuron* **42**, 522–524.
- Dawson VL, Dawson TM, Filloux FM & Wamsley JK (1988). Evidence for dopamine D-2 receptors on cholinergic interneurons in the rat caudate-putamen. *Life Sci* **42**, 1933–1939.
- Dell'Acqua ML, Smith KE, Gorski JA, Horne EA, Gibson ES & Gomez LL (2006). Regulation of neuronal PKA signaling through AKAP targeting dynamics. *Eur J Cell Biol* **85**, 627–633.
- Di Marzo V, Fontana A, Cadas H, Schinelli S, Cimino G, Schwartz JC & Piomelli D (1994). Formation and inactivation of endogenous cannabinoid anandamide in central neurons. *Nature* **372**, 686–691.
- Ding L, Perkel DJ & Farries MA (2003). Presynaptic depression of glutamatergic synaptic transmission by D1-like dopamine receptor activation in the avian basal ganglia. *J Neurosci* **23**, 6086–6095.
- Dumartin B, Doudnikoff E, Gonon F & Bloch B (2007). Differences in ultrastructural localization of dopaminergic D1 receptors between dorsal striatum and nucleus accumbens in the rat. *Neurosci Lett* **419**, 273–277.
- Dunwiddie TV & Masino SA (2001). The role and regulation of adenosine in the central nervous system. *Annu Rev Neurosci* **24**, 31–55.
- Geldwert D, Norris JM, Feldman IG, Schulman JJ, Joyce MP & Rayport S (2006). Dopamine presynaptically and heterogeneously modulates nucleus accumbens medium-spiny neuron GABA synapses in vitro. *BMC Neurosci* **7**, 53.
- Gorelova N & Yang CR (1997). The course of neural projection from the prefrontal cortex to the nucleus accumbens in the rat. *Neuroscience* **76**, 689–706.
- Goto Y & Grace AA (2007). The dopamine system and the pathophysiology of schizophrenia: a basic science perspective. *Int Rev Neurobiol* **78C**, 41–68.
- Grueter BA, Brasnjo G & Malenka RC (2010). Postsynaptic TRPV1 triggers cell type-specific long-term depression in the nucleus accumbens. *Nat Neurosci* **13**, 1519–1525.
- Hardingham GE, Arnold FJ & Bading H (2001). A calcium microdomain near NMDA receptors: on switch for ERK-dependent synapse-to-nucleus communication. *Nat Neurosci* **4**, 565–566.
- Harvey J & Lacey MG (1996). Endogenous and exogenous dopamine depress EPSCs in rat nucleus accumbens in vitro via D1 receptors activation. *J Physiol* **492**, 143–154.
- Harvey J & Lacey MG (1997). A postsynaptic interaction between dopamine D1 and NMDA receptors promotes presynaptic inhibition in the rat nucleus accumbens via adenosine release. *J Neurosci* **17**, 5271–5280.
- Higley MJ & Sabatini BL (2010). Competitive regulation of synaptic Ca²⁺ influx by D2 dopamine and A2A adenosine receptors. *Nat Neurosci* **13**, 958–966.
- Howlett AC (2005). Cannabinoid receptor signaling. *Handb Exp Pharmacol*, 53–79.
- Hsu KS, Huang CC, Yang CH & Gean PW (1995). Presynaptic D2 dopaminergic receptors mediate inhibition of excitatory synaptic transmission in rat neostriatum. *Brain Res* **690**, 264–268.
- Huang YH, Ishikawa M, Lee BR, Nakanishi N, Schluter OM & Dong Y (2011). Searching for presynaptic NMDA receptors in the nucleus accumbens. *J Neurosci* **31**, 18453–18463.
- Husi H, Ward MA, Choudhary JS, Blackstock WP & Grant SG (2000). Proteomic analysis of NMDA receptor-adhesion protein signaling complexes. *Nat Neurosci* **3**, 661–669.
- Joshi PR, Wu NP, Andre VM, Cummings DM, Cepeda C, Joyce JA, Carroll JB, Leavitt BR, Hayden MR, Levine MS & Bamford NS (2009). Age-dependent alterations of corticostriatal activity in the YAC128 mouse model of Huntington disease. *J Neurosci* **29**, 2414–2427.
- Kalivas PW & Volkow ND (2005). The neural basis of addiction: a pathology of motivation and choice. *Am J Psychiatry* **162**, 1403–1413.
- Karasawa J, Kotani M, Kambe D & Chaki S (2010). AMPA receptor mediates mGlu 2/3 receptor antagonist-induced dopamine release in the rat nucleus accumbens shell. *Neurochem Int* **57**, 615–619.
- Kearn CS, Blake-Palmer K, Daniel E, Mackie K & Glass M (2005). Concurrent stimulation of cannabinoid CB1 and dopamine D2 receptors enhances heterodimer formation: a mechanism for receptor cross-talk? *Mol Pharmacol* **67**, 1697–1704.
- Kramer PF, Christensen CH, Hazelwood LA, Dobi A, Bock R, Sibley DR, Mateo Y & Alvarez VA (2011). Dopamine D2 receptor overexpression alters behavior and physiology in Drd2-EGFP mice. *J Neurosci* **31**, 126–132.
- Kreitzer AC & Malenka RC (2005). Dopamine modulation of state-dependent endocannabinoid release and long-term depression in the striatum. *J Neurosci* **25**, 10537–10545.
- Laurenza A, Sutkowski EM & Seamon KB (1989). Forskolin: a specific stimulator of adenylyl cyclase or a diterpene with multiple sites of action? *Trends Pharmacol Sci* **10**, 442–447.
- Levine MS, Altemus KL, Cepeda C, Cromwell HC, Crawford C, Ariano MA, Drago J, Sibley DR & Westphal H (1996). Modulatory actions of dopamine on NMDA receptor-mediated responses are reduced in D1A-deficient mutant mice. *J Neurosci* **16**, 5870–5882.
- Lovinger DM (2010). Neurotransmitter roles in synaptic modulation, plasticity and learning in the dorsal striatum. *Neuropharmacology* **58**, 951–961.
- Lovinger DM & McCool BA (1995). Metabotropic glutamate receptor-mediated presynaptic depression at corticostriatal synapses involves mGluR2 or 3. *J Neurophysiol* **73**, 1076–1083.
- Manzoni OJ, Manabe T & Nicoll RA (1994). Release of adenosine by activation of NMDA receptors in the hippocampus. *Science* **265**, 2098–2101.
- Marcellino D, Carriba P, Filip M, Borgkvist A, Frankowska M, Bellido I, Tanganelli S, Muller CE, Fisone G, Lluís C, Agnati LF, Franco R & Fuxe K (2008). Antagonistic cannabinoid CB1/dopamine D2 receptor interactions in striatal CB1/D2 heteromers. A combined neurochemical and behavioral analysis. *Neuropharmacology* **54**, 815–823.
- Marsicano G, Goodenough S, Monory K, Hermann H, Eder M, Cannich A, Azad SC, Cascio MG, Gutierrez SO, van der Stelt M, Lopez-Rodriguez ML, Casanova E, Schutz G, Zieglerberger W, Di Marzo V, Behl C & Lutz B (2003). CB1 cannabinoid receptors and on-demand defense against excitotoxicity. *Science* **302**, 84–88.

- Maura G, Giardi A & Raiteri M (1988). Release-regulating D-2 dopamine receptors are located on striatal glutamatergic nerve terminals. *J Pharmacol Exp Ther* **247**, 680–684.
- Memo M, Missale C, Carruba MO & Spano PF (1986). Pharmacology and biochemistry of dopamine receptors in the central nervous system and peripheral tissue. *J Neural Transm Suppl* **22**, 19–32.
- Mennerick S & Zorumski CF (1995). Paired-pulse modulation of fast excitatory synaptic currents in microcultures of rat hippocampal neurons. *J Physiol* **488**, 85–101.
- Mizuno T, Schmauss C & Rayport S (2007). Distinct roles of presynaptic dopamine receptors in the differential modulation of the intrinsic synapses of medium-spiny neurons in the nucleus accumbens. *BMC Neurosci* **8**, 8.
- Neve KA, Seamans JK & Trantham-Davidson H (2004). Dopamine receptor signaling. *J Recept Signal Transduct Res* **24**, 165–205.
- Nicola SM, Kombian SB & Malenka RC (1996). Psychostimulants depress excitatory synaptic transmission in the nucleus accumbens via presynaptic D1-like dopamine receptors. *J Neurosci* **16**, 1591–1604.
- Nicola SM & Malenka RC (1997). Dopamine depresses excitatory and inhibitory synaptic transmission by distinct mechanisms in the nucleus accumbens. *J Neurosci* **17**, 5697–5710.
- Nicola SM, Surmeier J & Malenka RC (2000). Dopaminergic modulation of neuronal excitability in the striatum and nucleus accumbens. *Annu Rev Neurosci* **23**, 185–215.
- O'Donnell P & Grace AA (1994). Tonic D2-mediated attenuation of cortical excitation in nucleus accumbens neurons recorded in vitro. *Brain Res* **634**, 105–112.
- Pan B, Hillard CJ & Liu QS (2008). D2 dopamine receptor activation facilitates endocannabinoid-mediated long-term synaptic depression of GABAergic synaptic transmission in midbrain dopamine neurons via cAMP-protein kinase A signaling. *J Neurosci* **28**, 14018–14030.
- Pennartz CM, Groenewegen HJ & Lopes da Silva FH (1994). The nucleus accumbens as a complex of functionally distinct neuronal ensembles: an integration of behavioural, electrophysiological and anatomical data. *Prog Neurobiol* **42**, 719–761.
- Pickel VM, Chan J, Kearn CS & Mackie K (2006). Targeting dopamine D2 and cannabinoid-1 (CB1) receptors in rat nucleus accumbens. *J Comp Neurol* **495**, 299–313.
- Rebec GV (1998). Real-time assessments of dopamine function during behavior: single-unit recording, iontophoresis, and fast-scan cyclic voltammetry in awake, unrestrained rats. *Alcohol Clin Exp Res* **22**, 32–40.
- Reiner A, Albin RL, Anderson KD, D'Amato CJ, Penney JB & Young AB (1988). Differential loss of striatal projection neurons in Huntington disease. *Proc Natl Acad Sci U S A* **85**, 5733–5737.
- Sabatini BL, Oertner TG & Svoboda K (2002). The life cycle of Ca²⁺ ions in dendritic spines. *Neuron* **33**, 439–452.
- Seamans JK, Gorelova N, Durstewitz D & Yang CR (2001). Bidirectional dopamine modulation of GABAergic inhibition in prefrontal cortical pyramidal neurons. *J Neurosci* **21**, 3628–3638.
- Shuen JA, Chen M, Gloss B & Calakos N (2008). Drd1a-tdTomato BAC transgenic mice for simultaneous visualization of medium spiny neurons in the direct and indirect pathways of the basal ganglia. *J Neurosci* **28**, 2681–2685.
- Sulzer D (2011). How addictive drugs disrupt presynaptic dopamine neurotransmission. *Neuron* **69**, 628–649.
- Testa CM, Friberg IK, Weiss SW & Standaert DG (1998). Immunohistochemical localization of metabotropic glutamate receptors mGluR1a and mGluR2/3 in the rat basal ganglia. *J Comp Neurol* **390**, 5–19.
- Van der Kloot W (1991). The regulation of quantal size. *Prog Neurobiol* **36**, 93–130.
- Vanhoutte P & Bading H (2003). Opposing roles of synaptic and extrasynaptic NMDA receptors in neuronal calcium signalling and BDNF gene regulation. *Curr Opin Neurobiol* **13**, 366–371.
- Yin HH & Lovinger DM (2006). Frequency-specific and D2 receptor-mediated inhibition of glutamate release by retrograde endocannabinoid signaling. *Proc Natl Acad Sci U S A* **103**, 8251–8256.

Author contributions

Conception and design of the experiments: N.S.B. Collection, analysis and interpretation of data: D.D., W.W., J.L., A.B., E.K.E., I.N., J.T., G.P.S. and N.S.B. Drafting the article or revising it critically for important intellectual content: N.S.B. All authors approved the final version of the manuscript.

Acknowledgements

We would like to acknowledge Michael S. Levine, Carlos Cepeda and Gowry Fernando at the University of California, Los Angeles for providing breeding pairs of Drd1 and Drd2 EGFP BAC transgenic mice. We thank Nephi Stella and Xiaocui Sun at the University of Washington for providing CB₁-null and control mice. We thank David Sulzer, Richard Palmiter and David Perkel for careful reading and pertinent comments. We also thank Ian J. Bamford and Lisa H. Zimberg for assistance. This work was supported by NIH grants NS052536, NS060803, DA007278, and HD02274, the University of Washington Vision Research Centre and Seattle Children's Hospital, Seattle, WA.